University of Stavanger

FACULTY OF SCIENCE AND TECHNOLOGY

Master's Thesis

Study program/specialization: **Petroleum Engineering/ Drilling Technology**	Spring/Autumn semester, 2023 Open
Author: **Ugonna Gabriel Okeke**	……**Ugonna Gabriel Okeke**……. (Signature of author)
Program coordinator: Supervisor(s): **Mesfin Belayneh**	
Title of bachelor's thesis: ***Effect of fluid viscosity, lubricity, and fibre on the bridging performance of Quartz particle: Lost circulation experimental study***	
Credits: 30	
Keywords: Quartz Fiber Lubricity Lost circulation Rheological parameters Bridging	Number of pages: 87 + Supplemental material/other: 3 Date/year 15/05/2023 Stavanger

ACKNOWLEDGEMENTS

I am sincerely grateful to my supervisor, **Mesfin Belayneh**, for his invaluable guidance, support, and expertise throughout my master's thesis. His dedication and belief in my abilities have shaped the outcome of this work.

I also extend heartfelt thanks to my beloved, **Klaudia Anna Czepiel**, for her unwavering support, understanding, and sacrifices which have made it possible for me to pursue my academic aspiration.

ABSTRACT

This master's thesis delves into the investigation of the influential factors that affect the lost circulation material's bridging performance at a fracture gate. The study begins by examining the quartz particles bridging performance at different fracture widths, followed by the investigation of the drilling fluids' viscosity and lubricity impacts on the particles bridging stability behavior. Additionally, the study assesses the potential enhancement of quartz performance through fiber reinforcement.

The research findings reveal that the incorporation of fibers indeed improves the bridging performance of quartz particles. Moreover, an intriguing trend emerges when examining the effect of viscosity on bridging performance. The analysis considers the Bingham Plastic, Power Law, and Herschel-Buklkey's rheological parameter. Results exhibited that an increase in these parameters correlates with a rise in the average bridging pressure across different selected slot sizes.

Furthermore, the study investigates the impact of lubricity by comparing the coefficient of friction (COF) between two selected fluids. The test results showed that the fluid with a higher COF (less lubricity) demonstrates better particle bridging stability when compared with the fluid exhibiting a lower COF (high lubricity).

In summary, this research emphasizes the crucial role of fiber reinforcement in enhancing the bridging performance of quartz particles. Additionally, it highlights the notable effects of viscosity and lubricity on bridging behavior, providing valuable insights for optimizing and improving the performance of quartz-based systems.

TABLE OF CONTENTS

LIST OF FIGURES

LIST OF TABLES

LIST OF ABBREVIATIONS

API = American Petroleum Institute

AV Apparent viscosity

BHP = Bottom hole pressure

Bbl = barrel

DF = Drilling fluid

ECD = Equivalent circulating density

FCS = Fracture closure stress

HPHT = High pressure high temperature

IPT = Ideal packing theory

LCM = Lost circulation material

MW = Mud weight

MPa = Mega pascal

Na = Sodium

NP = Nanoparticle

NPT = Non-productive time

OBM = Oil-based drilling fluids

PSD = Particle size distribution

PV = Plastic viscosity

PDC = Polycrystalline diamond compacts

RPM or rpm = Revolutions per minute

ROP = Rate of penetration

TVD = True vertical depth

UIS = University of Stavanger

WBM = Water-based drilling fluids

WSM = Wellbore strength material

Wt% = Weight percent

YP =Yield point

LIST OF SYMBOLS

A = cross-sectional area of specimen (mm^2)

ρ= density (kg/m^3)

τ = Shear stress (Pa)

τ_c = Yield stress (Pa)

μ_c = Viscosity (Pa.s)

γ = Shear rate (sec^{-1})

µm = micrometer

µ = Viscosity [cP]

k = Consistency index [lbf s^n/100sqft]

n = Flow index [dimensionless]

r = Radius [m]

t = Time [s]

v = Velocity [m/s]

F = Applied Force [N]

1 INTRODUCTION

Wellbore instability has been and still is a challenging issue for the oil and gas industry. Drilling operations become difficult in environments such as depleted formations, horizontal wells, and deep-water environments where the operational windows are narrow, where the wellbore instability (collapse, and fracturing) and lost circulation are common problems. Moreover, drilling in high fracture also results in lost circulation problems, which increases both operational and non-productive time significantly.

This MSc thesis presents the bridging performance of biodegradable fiber materials in Bentonite drilling fluid. the study also investigates the impact of lubricity and rheological parameters on the bridging pressure.

1.1 Background

Lost circulation occurs when drilling fluid flows uncontrollably into the formation, resulting in several undesired consequences that significantly increase the non-productive time (NPT) during well drilling. This can incur substantial financial costs for the operating company [4]

To further emphasize this, A study conducted by [5] on the Brent field in the Viking Graben of the northern North Sea has been reviewed. The study examined lost circulation problems related to the field. The cause was attributed to the narrowing of the mud weight window due to reservoir depletion gradually reducing the fracture gradient. To address this, attempts were made to conduct underbalanced drilling by lowering the mud weight by 700-900 psi below the shale pore pressure. Two case histories revealed the possibility of drilling through the shale underbalanced; however, liner hang-up occurred in both cases due to shale collapse. The study revealed that Reservoir depletion in this field had reached a point where the minimum mud weight required for shale stability nearly equaled the fracture propagation pressure for the reservoir sands. In the first half of 2002, five out of seven wells drilled experienced lost circulation, resulting in a noteworthy non-productive time (NPT) an average of 300 hours per well. Although the problem was resolved by introducing a specified concentration of graphite (LCM) to the oil-based mud, during ten field trials, all sections reached total depth (TD) without

inducing losses. However, four out of the ten sections did experience losses during liner running and/or circulation before cementing [5]

Furthermore, [6] reported that approximately one-third of the incidents contributing to NPT can be attributed to lost circulation. J. Cook et al. also noted that well integrity issues, such as stuck pipe, wellbore collapse, sloughing shales, and lost circulation, accounted for up to 44% of NPT in the Gulf of Mexico alone. Due to the significant financial implications of well integrity-related NPT, operators may allocate an additional 10% to 20% of the overall drilling cost to account for anticipated downtime [7]

Based on the aforementioned reviewed case, it is evident that lost circulation plays a substantial role in NPT and is poised to become an even greater contributor in the future. Several experimental studies have been conducted to combat lost circulation, with the most common method involving the application of lost circulation materials (LCMs) in the drilling fluid to prevent filtrate loss by forming a bridge at the fracture opening.

The University of Stavanger has undertaken numerous studies on lost circulation, including an investigation into the bridging performance of LC-Lube and Mica, as well as their blending in 80/20 and 60/40 oil-based drilling fluids. This study provides valuable contextual information for current studies.

This thesis goes beyond the existing research by examining the performance of Quartz as a Lost Circulation Material (LCM) when combined with fiber. Furthermore, it aims to establish a correlation between fluid rheology parameters and bridging pressure, Additionally, the impact of lubricity on bridging performance is also a key aspect explored in this study.

1.2 Objectives

The objective of this thesis is to examine the impact of fluid viscosity, lubricity, and fiber on the bridging performance of Quartz particles in the context of lost circulation during drilling operations. The study focuses on the behavior of Quartz particles as Lost Circulation Materials (LCMs) in bentonite-based drilling fluids and their interaction with rheological parameters, lubricity, and fiber additives. It is important to note that the study has certain limitations, including experiments conducted under static conditions using a static bridging apparatus. However, the findings of this investigation will enhance our understanding of the underlying

mechanisms involved in lost circulation events and provide valuable insights for future research and practical applications.

1.3 Research methods

To achieve the stated objective, the methods employed in this thesis project are summarized in Figure 1.1. The initial part encompasses a literature study on lost circulation mitigation methods, classification, and field case studies utilized for managing lost circulation. The detailed activities related to experimentation and data analytics are outlined below:

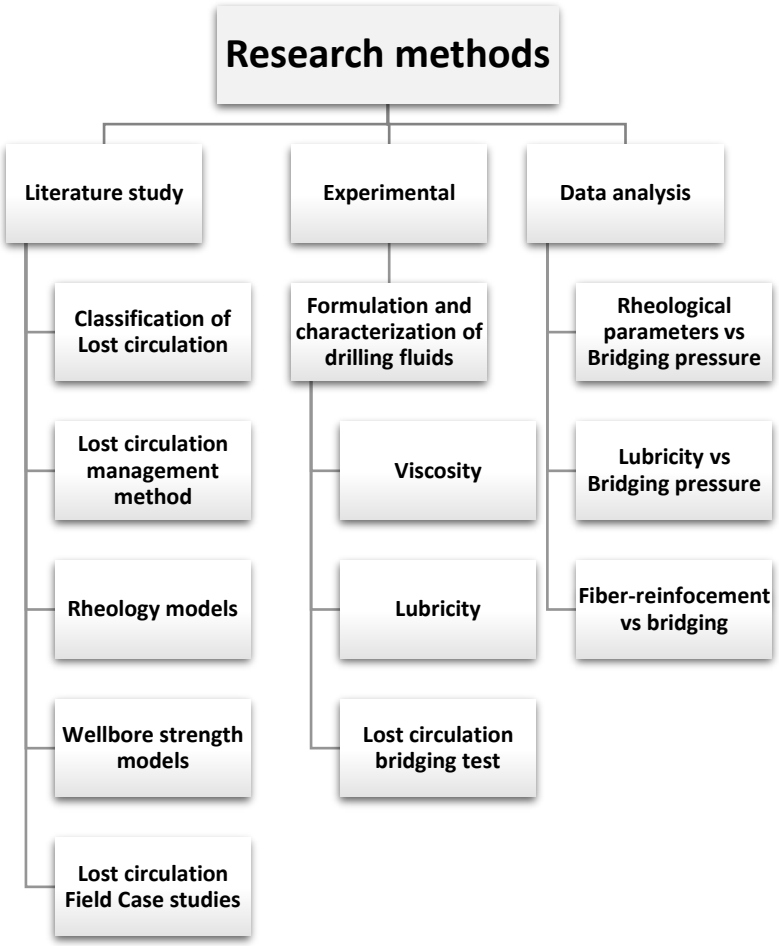

Figure 1.1 Research Method

1. ***Experimental Design***: The experimental design involved conducting tests using a static bridging apparatus to simulate lost circulation scenarios. The apparatus was set up to replicate drilling fluid flow conditions and the formation of a bridge. The experiments were performed in a controlled environment to accurately measure and analyze the performance of Quartz particles as LCMs.

2. ***Sample Preparation:*** Two types of Bentonite-based drilling fluids were prepared to capture different operational conditions encountered in drilling operations. The first type represented a more realistic drilling fluid, closely resembling field conditions. The second type, intentionally designed to study the effect of viscosity and lubricity, represented a less realistic fluid. Systematic adjustments were made to the viscosity and lubricity levels of both fluids to simulate a range of operational scenarios. Additionally, fiber additives were incorporated into the fluid systems to evaluate their influence on particle stability and bridge formation. This comprehensive sample preparation approach allowed for a thorough analysis of the impact of fluid properties on the bridging performance of Quartz particles.
3. ***Bridging Performance Evaluation:*** The bridging performance of Quartz particles was evaluated by measuring the bridging pressure exhibited by the fluid system. The bridging pressure was determined by gradually increasing the pressure applied to the fluid while monitoring the formation and stability of the bridge. The data obtained allowed for the quantitative assessment of bridging performance and its correlation with fluid properties.
4. ***Rheological Analysis:*** The rheological properties of the drilling fluids were analyzed using viscometry and rheometry techniques. The fluid viscosity, yield stress, and other relevant rheological parameters were measured to establish correlations with bridging pressure and assess the influence of fluid properties on lost circulation prevention.
5. ***Data Analysis:*** The collected data, including bridging pressure measurements, fluid rheological properties, and observations of bridge stability, were analyzed using statistical methods. Correlation analysis was performed to identify potential relationships between fluid parameters and bridging performance. The results were then interpreted to draw meaningful conclusions and validate the research objectives.

It is important to note that the experiments were conducted under static conditions on a static bridging apparatus. While this limitation restricts the representation of dynamic drilling scenarios, the controlled experimental setup allowed for focused investigation and analysis of the specific factors under examination.

2 Literature Review

This chapter provides a concise review of key concepts related to lost circulation, encompassing essential topics such as drilling fluid and its classification, fundamental principles of lost circulation, fluid rheology and characterization, as well as other relevant concepts and models. This section aims to offer a succinct and informative overview that clarifies the theories and mechanisms underlying lost circulation phenomena. By exploring these concepts, a solid foundation is established for the subsequent discussion and analysis of lost circulation-related issues.

2.1 Drilling Fluid

Drilling fluids, also known as drilling muds, refers to a specialized fluid used during the drilling process to facilitate the extraction of oil and gas resources from underground reservoirs. They are carefully engineered to meet the specific requirements of each drilling operation, taking into consideration factors such as well depth, formation characteristics, and drilling objectives.

In drilling operations, drilling fluids are circulated from the surface through the wellbore as is shown in figure 2.1 Their primary purpose is to enable cost-effective and efficient drilling, ensuring the creation of a stable and accurately gauged borehole that reaches the desired target depth while minimizing the risk of damage to prospective formations [8].
Additional functions of drilling fluids are outlined below.

2.1.1 Functions of Drilling fluids.

Drilling fluids serve various essential functions throughout the drilling process, including:

1. ***Formation Stabilization***: Drilling fluids exert pressure against the formation walls, providing stability to prevent the collapse of the wellbore. This is achieved by maintaining an appropriate hydrostatic pressure, which counters the formation pressure and prevents unwanted influxes.
2. ***Cuttings Transport***: Drilling fluids carry the drilled rock cuttings from the bottom of the wellbore to the surface. This transport occurs through the annulus, the space between the drill string and the wellbore wall. The drilling fluids carry the cuttings through the annulus, and they are subsequently processed and separated from the fluid at the surface using equipment such as degassers, desilters, and desanders.

3. ***Cooling and Lubrication***: Drilling fluids aid in cooling the drill bit and reducing friction between the bit and the formation. This cooling and lubricating effect helps to prevent overheating and wear on the drilling equipment.
4. ***Pressure Control***: Drilling fluids assist in maintaining wellbore pressure at an appropriate level, preventing the uncontrolled flow of formation fluids or gases. This is accomplished by adjusting the density and rheological properties of the drilling fluid to balance the formation pressure [9].

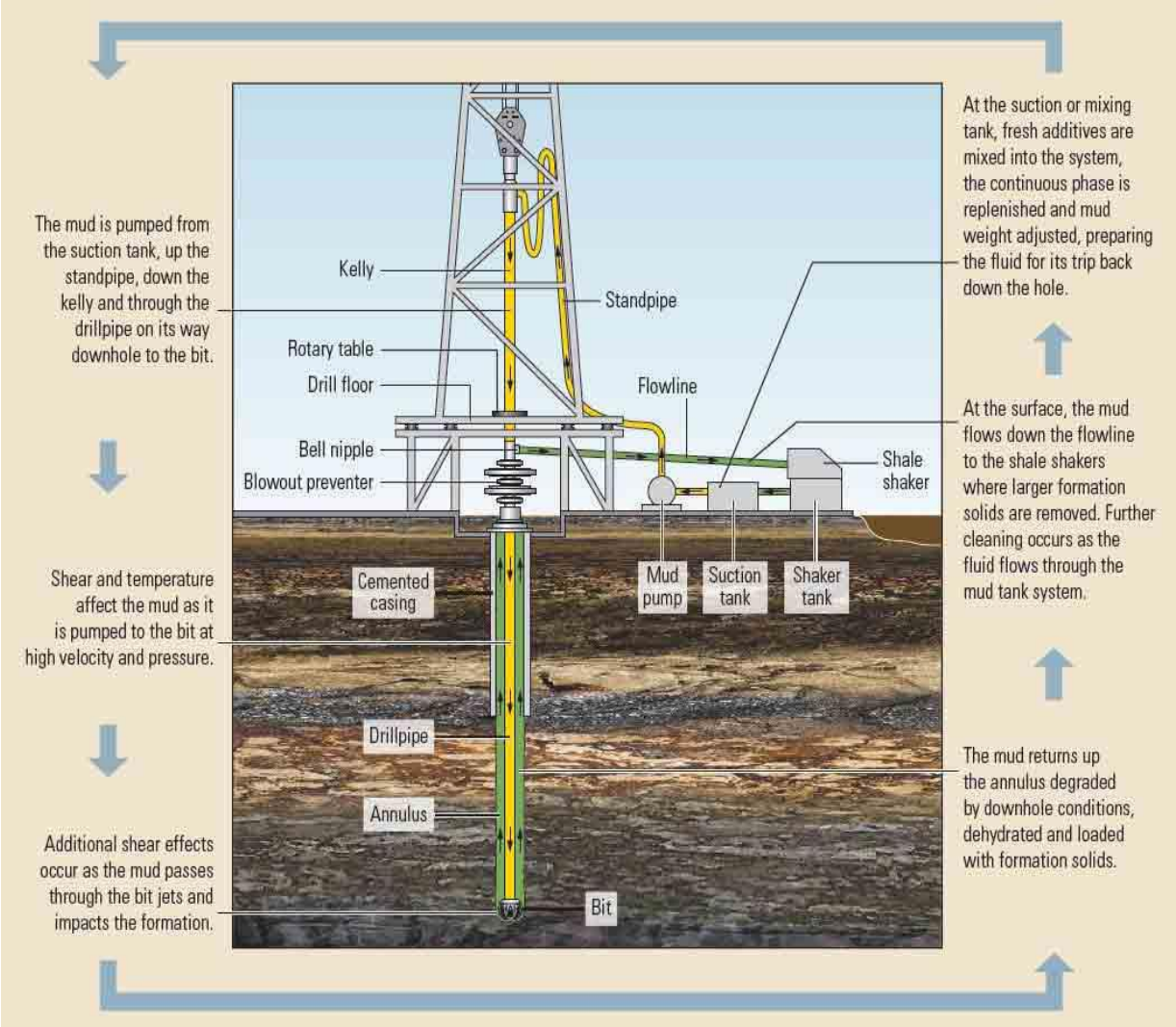

Figure 2.1: A Conventional circulation system; source:[2]

2.1.2 Drilling Fluid Classification.

Drilling fluids can be classified into various types based on their composition, which typically includes a base fluid and additives. The base fluid can be water-based (water as the continuous phase), oil-based (oil as the continuous phase), or synthetic-based (synthetic compounds as the continuous phase). Additives are incorporated into the base fluid to enhance specific properties such as density, viscosity, lubricity, filtration control, shale stability, and wellbore strengthening. Each category offers distinct advantages and is selected based on geological formations, wellbore stability requirements, and environmental considerations [10].

1. ***Water-Based Muds (WBM)***: Water-based muds are the most commonly used drilling fluids due to their cost-effectiveness and versatility. These fluids are primarily composed of water, along with various additives and solids. The classification of water-based muds can be further categorized into three subtypes:[11]

   a*) Freshwater Muds*: These muds utilize freshwater as the base fluid. They are suitable for drilling shallow wells and formations that do not react unfavorably with water.

   b) *Saltwater Muds*: Saltwater muds employ saline water, such as seawater or saturated salt solutions, as the base fluid. They are used in offshore drilling or in regions where freshwater availability is limited.[12]

   c*) Inhibited Water-Based Muds*: Inhibited water-based muds contain additives to control the reactivity of clay minerals and prevent the swelling or dispersion of formations. These fluids are commonly used in areas with shale formations.[13]

2. ***Oil-Based Muds (OBM)***: Oil-based muds are formulated by blending a base oil, typically diesel or mineral oil, with additives and solids. They offer superior lubricity, thermal stability, and shale inhibition compared to water-based muds[14]. Oil-based muds are further classified into two types:

   a) *Low Toxicity Oil-Based Muds (LTOBM*): LTOBMs are designed to minimize environmental impact while maintaining the desired performance. They employ less toxic or biodegradable base oils and carefully selected additives.

b) *Synthetic Oil-Based Muds (SOBM)*: SOBMs utilize synthetic base oils, such as esters or olefins, to enhance their performance and environmental compatibility. These fluids are commonly used in environmentally sensitive areas or challenging drilling conditions.

3. ***Synthetic-Based Muds (SBM)***: Synthetic-based muds combine the advantages of both water-based and oil-based muds. They utilize a blend of synthetic base fluids, additives, and solids. SBMs offer excellent thermal stability, lubricity, and environmental compatibility. They are further classified into two subtypes:

   a) *Water-In-Oil (W/O) SBMs*: W/O SBMs have water as the dispersed phase within the continuous oil phase. They exhibit excellent shale stability and are suitable for highly reactive shale formations.

   b) *Oil-In-Water (O/W) SBMs*: O/W SBMs have oil as the dispersed phase within the continuous water phase. They provide improved hole cleaning and cuttings transport capabilities[15].

Drilling fluids that do not fall into the above-mentioned categories are classified as "other fluids." This category includes foam-based fluids, air/mist drilling fluids, and inert gas drilling fluids. Understanding the characteristics and classifications of drilling fluids is crucial for engineers to optimize drilling operations and ensure safe and efficient wellbore construction. To enhance this understanding, the following section provides a concise introduction to fluid rheology, which explains the flow behavior of drilling fluids.

2.2 Fluid Rheology.

Rheology is a scientific field that focuses on the study of how fluids flow and deform. In the context of drilling fluids, rheology plays a crucial role in monitoring and understanding the changes in fluid properties under downhole conditions. These conditions can significantly impact drilling efficiency and safety. The Key rheological properties of drilling fluids discussed in this thesis include yield point, gel strength, and viscosity, which can be further classified into apparent and plastic viscosity. By effectively controlling these properties, the drilling process can be optimized to minimize risks and maximize productivity [16]

2.2.1 Viscosity

Viscosity is a fundamental physical property that characterizes a fluid's resistance to flow when subjected to shear stress. It represents the internal friction within a fluid that resists changes in its shape or form. Viscosity is an essential parameter in various industries, including lubrication, transportation, and manufacturing processes. It plays a critical role in controlling the flow of liquids in applications such as injection molding, surface coating, and spraying[17]. Mathematically, viscosity is defined as the ratio of shear stress to shear rate [18]

$$\mu = \tau / \gamma \tag{2.1}$$

Where: μ is the viscosity, τ is the shear stress, and γ is the shear rate. The unit of viscosity depends on the system of measurement being used. In the International System of Units (SI), viscosity is measured in Pascal-seconds (Pa·s) or, more commonly, in centipoise (cP) in non-SI units.

2.2.2 Shear Stress

Shear stress in drilling fluid refers to the force per unit area required to maintain a constant flow rate. It is a measure of the resistance encountered when fluid layers move relative to each other.[19]

2.2.3 Shear Rate

Shear rate is defined as the gradient of the velocity of the fluid flow. It is determined by the flow's geometry and speed and is a crucial factor in understanding fluid behavior [20].

2.2.4 Plastic Viscosity

Plastic viscosity is a measure of a fluid's resistance to flow due to the internal mechanical friction between its components, which include both solid and liquid constituents. It characterizes the flow behavior of certain fluids, particularly non-Newtonian fluids like drilling mud or certain types of plastics.

2.2.5 Yield Point

In drilling fluids, the yield point represents the resistance to initial fluid flow, specifically the stress required to initiate movement. It is a parameter in the Bingham plastic model. The unit of yield point is typically expressed in Pascal (Pa) or other pressure units depending on the system of measurement used [21].

2.2.6 Gel Strength

Gel strength characterizes a drilling fluid's ability to resist flow when it is at rest. It is typically determined by measuring the force required to initiate fluid movement after a specified period of rest. The units of gel strength depend on the system of measurement being used. Common units include Pascal (Pa) or pound-force per square inch (lbf/in^2). High gel strength is desirable in challenging drilling conditions to prevent fluid loss into porous formations, which can lead to lost circulation, increased costs, and safety concerns.

To maintain effective gel strength, drilling fluids are formulated with additives such as polymers, clays, and other chemical compounds. These additives enhance the strength of the gel, improve its ability to suspend and transport drilling cuttings, and maintain wellbore stability[22].

2.3 Rheology Models

Rheological models play a crucial role in the comprehensive analysis of drilling fluid behavior under dynamic conditions. Accurate modeling of drilling mud characteristics relies on the appropriate selection of a rheological model that closely aligns with the observed rheological data of the fluid being investigated. This study primarily focuses on non-Newtonian models as they provide the most accurate representation of drilling fluid properties.

2.3.1 Newtonian Fluids

Newtonian fluids are characterized by a direct proportionality between the rate of deformation, known as shear rate, and the resulting shear stress. In simpler terms, Newtonian fluids exhibit a linear relationship between shear stress and shear rate, with viscosity being the constant of proportionality [23].

Mathematically, the relationship between shear stress (τ), viscosity (μ), and shear rate (γ) for a Newtonian fluid can be described by the equation:

$$\tau = \mu \times \gamma \tag{2.2}$$

It is important to note that this relationship holds true only for Newtonian fluids, where the viscosity remains consistent regardless of the applied shear stress or shear rate. Examples of Newtonian fluids include water, air, alcohol, gasoline etc.. These fluids possess the characteristic of flowing easily and predictably, making them highly suitable for various industrial and scientific applications [24]

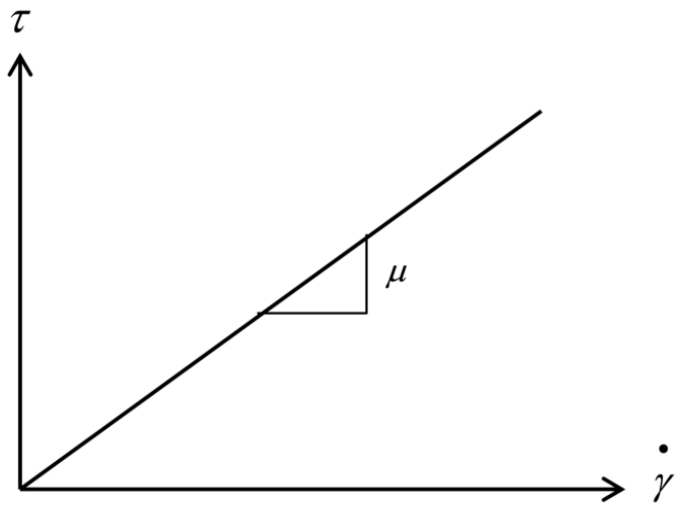

Figure 2.2 Flow curve of a Newtonian fluid [25]

2.3.2 Non-Newtonian Fluids

Non-Newtonian fluids, including drilling fluids used in the oil industry, exhibit a non-linear relationship between shear stress and shear rate. Their viscosity undergoes changes when subjected to external forces [26]

In drilling operations, the viscosity of drilling fluids decreases in the drill string due to high shear rates, resulting in reduced circulating pressures. Conversely, in the annulus, where shear rates are lower, the mud viscosity remains high, facilitating efficient transportation of drill cuttings. During circulation pauses, drilling fluids form a gel-like consistency, aiding in the suspension of cuttings and solids [27]

Drilling fluids are commonly classified as shear-thinning fluids, characterized by a decrease in viscosity as the shear rate increases. Several rheological models are available to describe the relationship between shear rate and shear stress for such fluids. In this thesis, we will utilize the Bingham, Power law, Herschel-Bulkley, and Robertson and Stiff rheological models to quantify the rheological parameters of the generated drilling fluids. The following section offers a concise overview of these models.

2.3.2.1 Bingham Plastic Model

The Bingham plastic model is widely used in the drilling industry due to its simplicity, although it may not accurately depict the behavior of drilling fluids under extremely low (in the annulus) or high shear rates (at the bit)[18]

According to this model, flow initiates only when the applied force surpasses a specific level known as yield stress. This concept is visually represented in figure 2.3. Mathematically, it can be described as:

$$\tau = YS + PV\gamma \tag{2.3}$$

Where: τ represents the shear stress, YS denotes the yield point, PV signifies the plastic viscosity, and γ represents the shear rate.

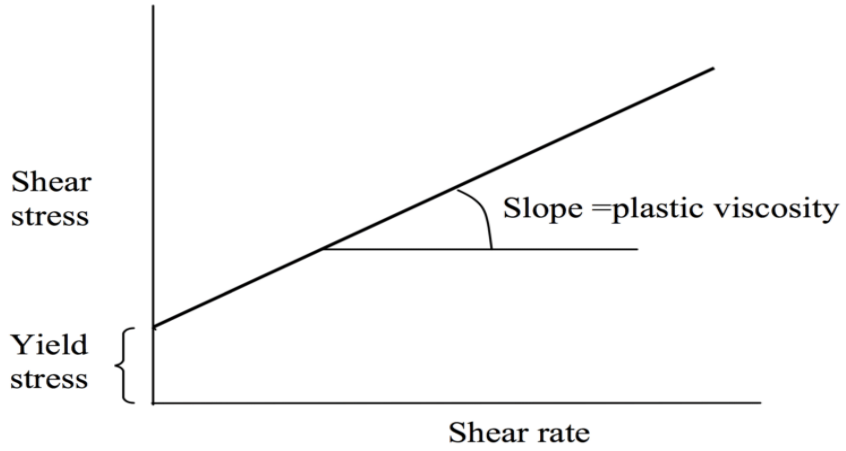

Figure 2.3: Bingham plastic Model [28]

The Bingham parameters, namely the plastic viscosity (PV) and the yield stress (YS), can be determined either by reading them directly from a graph or by calculating them using the following equations:

$$PV\ (cP) = R600 - R300 \tag{2.4}$$

$$YS\ (lbf/100sqft) = R300 - \mu p \tag{2.5}$$

Here, R600 and R300 represent certain values obtained from the analysis or measurement of the fluid, while μp denotes another parameter associated with the plastic viscosity [18]. These equations allow for the quantification of the Bingham parameters required for characterizing the rheological behavior of the fluid.

2.3.2.2 Power Law

The power law model is commonly employed to characterize the rheological behavior of shear-thinning fluids, such as polymer and foam solutions [29] Unlike the Bingham plastic model, which assumes a linear correlation between shear stress and shear rate, the power law model provides a more accurate representation of drilling fluid. It describes the flow behavior of fluids using a power-law relationship between shear stress and shear rate. This model captures a wider range of flow behavior, including shear-thinning or shear-thickening properties observed in drilling fluids. Specifically, the power law states that the shear stress is proportional to the shear rate raised to a certain power, known as the flow behavior index.[18].

$$\tau = k\gamma^n \tag{2.6}$$

Where:

- τ = Shear stress
- k = consistency index
- γ = shear rate
- n = flow behavior index

The k and n index parameters can be estimated from the equation below.

$$n = 3.32 \log\left(\frac{R_{600}}{R_{300}}\right) \tag{2.7}$$

$$k = \frac{R_{300}}{511^n} = \frac{R_{600}}{1022^n} \tag{2.8}$$

The flow behavior index can define the level of the non-Newtonian behavior and can take three set of values:

- If n = 1 the fluid is considered as Newtonian
- If n<1 the fluid is considered as non-Newtonian
- If n>1 the fluid is considered as Dilatant

The constant 'K' is a consistency index and gives the level of the fluid thickness, the higher the K value, the thicker the fluid [27].

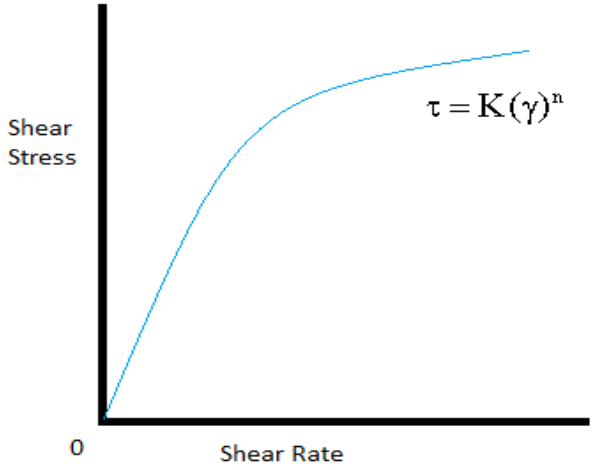

Figure 2.4: Power law Model

2.3.2.3 Herschel-Bulkley Model

The Herschel-Bulkley model, also known as the yield-power law model, offers a more accurate description of mud rheology compared to the Bingham plastic and power law models. This model encompasses the entire range of shear rates, providing a comprehensive characterization of mud behavior, as mentioned in the source by [30]

The Herschel-Bulkley model states that a fluid necessitates external pressure to initiate flow at zero shear strain, and as the shear rate increases, the viscosity decreases.

Mathematically, the model consists of three parameters and is expressed as:

$$\tau = \tau_y + k\gamma^n \tag{2.9}$$

Where

- τ = shear stress
- τ_y = yield stress
- k = consistency index

- γ = shear rate
- n = flow index

The parameters n and k can be determined graphically, while τ_0 can be calculated using the equation below [30].

$$\tau_0 = \frac{\tau^{*2} - \tau_{min} \cdot \tau_{max}}{2\tau^{*} - \tau_{min} - \tau_{max}} \quad (2.10)$$

The parameter $\tau^*$is determined from the corresponding geometric average value of shear rate, γ^*, which can be determined from [30]:

$$\gamma^* = \sqrt{\gamma_{min}\gamma_{max}} \quad (2.11)$$

Below is a graphical representation of the Herschel-Bulkley model.

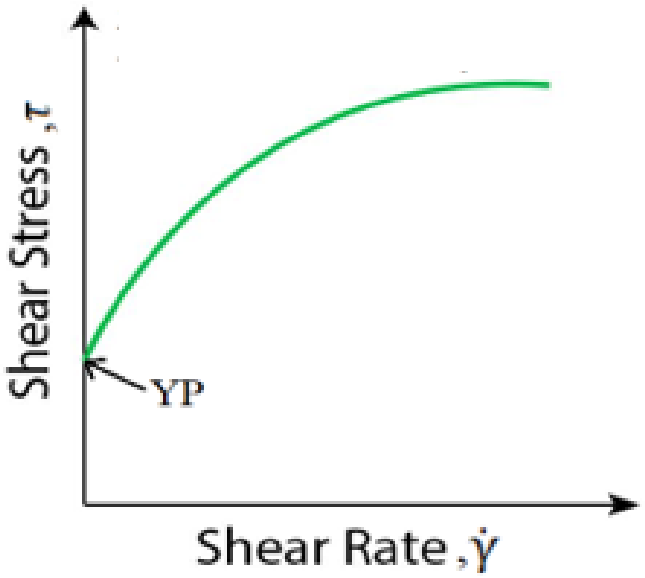

Figure 2.5: Shear stress-shear rate relationship of Herschel Bulkley Model [27]

2.3.2.4 Robertson and Stiff Model

The Robertson and Stiff model is utilized to describe the rheological behavior of drilling fluids and cement slurries. This model offers several key advantages, as stated by [19]

The advantages claimed for this model are as follows:

1. Provides a better fit for rheological data compared to other three-parameter models.
2. Offers explicit relationships for velocity fields, wall shear rates, and flow rate/pressure drop relations in tube and annular flows.

The basic equation of the Robertson and Stiff model is as follows [30] .:

$$\tau = A(\gamma + C)^B \tag{2.12}$$

Where:

- A, B and C are model parameters.
- τ = shear stress
- γ = shear rate

The parameters A and B can be considered similar to k and n parameters in the power law. The term $(\gamma + C)$ is considered as effective shear rate. The parameter C is a correction factor to the shear rate γ, and is estimated from the equation below [30].

$$C = \frac{\gamma_{min} \cdot \gamma_{max} - \gamma^{*2}}{2\gamma^{*} - \gamma_{min} - \gamma_{max}} \tag{2.13}$$

Here, $\gamma*$ represents the shear rate value corresponding to the geometric mean of the shear stress, $\tau*$ [30].

The geometric mean of the shear stress ($\tau*$) is then calculated from:

$$\tau^{*} = \sqrt{\tau_{min}\tau_{max}} \tag{2.14}$$

2.4 Lost Circulation fundamentals.

Lost circulation events during drilling operations often occur as a result of the drilling methodology employed. Conventionally, wells are drilled in an overbalanced manner, where the hydrostatic pressure within the well is maintained above the pore pressure of the formation. The control of hydrostatic pressure is achieved through the use of drilling mud with specific density properties, as discussed by [31].

The advantages of drilling in an overbalanced manner include:

- Prevention of uncontrolled influx of formation fluids, which, in rare cases, could lead to a blowout, posing risks to wellhead equipment and potential harm to rig personnel.
- Maintenance of wellbore stability and prevention of wellbore collapse by keeping the wellbore in proper gauge.

However, drilling with an excessively high mud weight can result in hydrostatic pressure that exceeds the fracture gradient of the formation. This can cause the formation to fracture, allowing drilling fluids to enter the formation through these newly created fractures. Formation

fracture occurs due to tensile failure around the wellbore, which happens when the stress exerted on the formation surpasses its tensile strength and the hoop stress around the wellbore [32].

The formation fracture gradient is determined through a pressure integrity test called an extended leak-off test (XLOT). This test is conducted immediately after drilling beneath the casing shoe of the previous well section. During an XLOT, the well is shut in, and fluid is pumped into the wellbore to incrementally increase the pressure exerted on the formation, as explained by [7]. Figure 2 illustrates a typical pressure plot obtained from an XLOT.

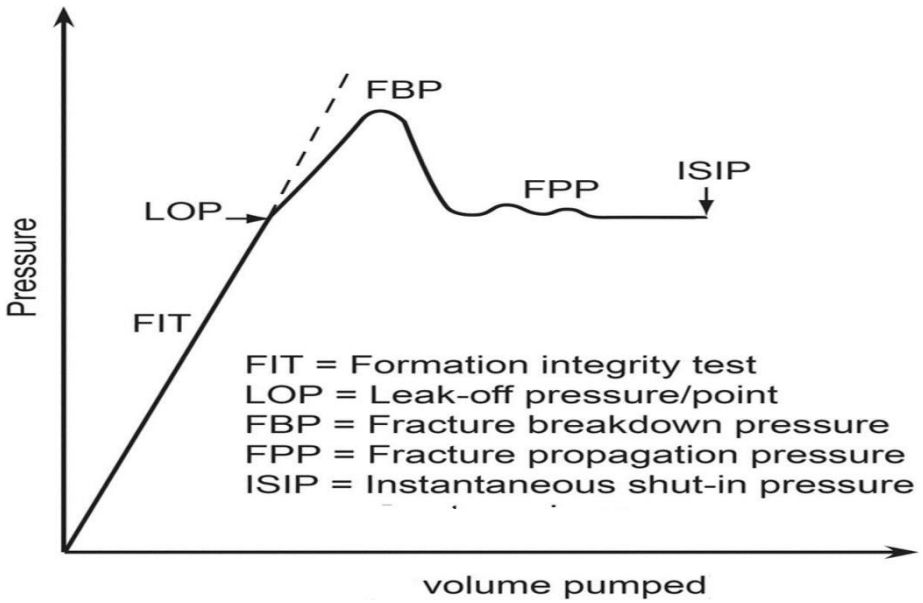

Figure 2.6: Extended leak off test plot

During the initial stages of the extended leak-off test (XLOT), the pressure in the wellbore demonstrates a linear relationship with the volume of fluid pumped. As more fluid is injected into the wellbore, the pressure continues to increase linearly until it reaches the point of leak-off, marking the departure from linearity (LOP). It is at this pressure point that a fracture initiation occurs. The fracture then propagates through the formation until it reaches the formation breakdown pressure (FBP). At this point, the pressure curve experiences a rapid drop-off, and the fractures continue to propagate in a more controlled manner at a lower and relatively steady pressure known as the fracture propagation pressure (FPP). Careful analysis of the pressure data obtained during the XLOT, can provide valuable information about the formation's characteristics, such as its fracture gradient, mechanical properties, and stability. This information is crucial for designing an effective wellbore stability strategy, selecting

appropriate drilling fluids, and implementing proper lost circulation prevention and control measures.[33]

2.4.1 The Fracturing Process

Fracturing in a well occurs when the hoop stress exerted around the wellbore surpasses the tensile strength of the formation. The magnitude of hoop stress is influenced by the pressure within the borehole. Understanding the processes involved in fracture initiation, growth, and filter cake formation is crucial for mitigating risks associated with lost circulation and maintaining well integrity.

A qualitative overview of the fracturing process, as described by [34]., is as follows:

1. **Filter Cake Formation**: The fracturing process begins with the development of a filter cake, which acts as a barrier between the drilling mud and the formation. As drilling mud flows, a thin filter cake gradually develops due to the loss of small volumes of filtrate into the formation. The thickness of the filter cake is determined by the balance between the attraction of filtrate and erosion caused by the flow.
2. **Fracture Initiation**: Increasing borehole pressure shifts the hoop stress from compression to tension. The continuous loss of filtrate from the well helps maintain the integrity of the filter cake, enabling it to support the in-situ stresses and resist the rising wellbore pressure until a critical pressure is reached, triggering the initiation of fractures.
3. **Fracture Growth**: With increasing wellbore pressure, the width of the fractures continues to expand. The mechanical strength of the filter cake particles contributes to the formation of a stress bridge across the fractures, which aids in the stability of the filter cake. During this phase, both the rock stress (in-situ stress) and the strength of the filter cake cooperate to prevent failure.
4. **Continued Fracture Growth**: As pressure further escalates, the fractures widen, and the stress bridge across the fractures weakens.
5. **Filter Cake Collapse**: At a critical pressure exceeding the yield strength of the particles, the filter cake loses its strength, and the "rock bridge" collapses. This leads to the establishment of communication between the borehole and the formation, resulting in mud losses in the formation [34].

Event	Fig	Main controlling parameters
Filter cake formation		Filtrate loss
Fracture initiation	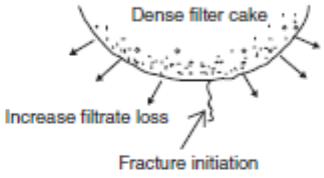	Filtrate loss, Stress
Fracture growth	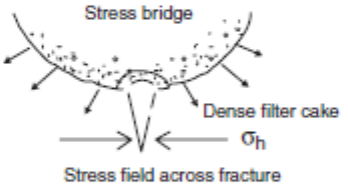	Bridge stress Rock stress
Further fracture growth	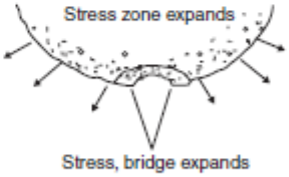	Bridge/rock stress Particle strength
Filter cake collapse	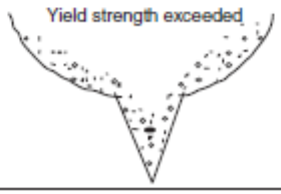	Particle strength

Figure 2.7 Qualitative description of the fracturing process.[34]

2.4.2 Potential Mud Loss Zones

Drilling fluids can be lost into the formation through fractures or openings. These fractures can be drilling-induced or naturally occurring, and understanding the factors contributing to mud loss in these zones is crucial for effective wellbore management [35].

2.4.2.1 Drilling-Induced Fractures

Drilling-induced fractures occur when the equivalent circulating density (ECD) exceeds the critical pressure for formation fracture. This can be attributed to various drilling practices, including improper hydraulics with excessive pump rates, rapid changes in pump rates during connections or trips (more common in oil-based muds due to temperature effects), surge/swab

caused by rapid pipe movement, inadequate hole cleaning, poor drilling fluid design, and pipe whipping [36]. Once a fracture is created, it can be challenging to repair, and the formation may never regain its original strength.

2.4.2.2 Naturally Occurring Fractures

Naturally occurring fractures refer to pre-existing fractures or fissures within the rock formations. These fractures are created through various geological processes such as tectonic movements, thermal stress, or chemical reactions and can act as pathways for drilling fluids to escape, leading to lost circulation-related problems. Preventing lost circulation in formations that are cavernous, vugular, fractured, or unconsolidated can pose significant challenges [37].

2.4.2.3 Highly Permeable and Coarse, Unconsolidated Formations:

In highly permeable and coarse, unconsolidated formations, drilling fluids can invade the formation matrix, leading to lost circulation. Such formations are commonly encountered in shallow sands and gravel beds. It is essential to prevent mud loss in these intervals as it can cause washout in unconsolidated zones, creating unstable large cavities that are susceptible to collapse under the overburden weight. Gradual mud level decline in tanks can serve as an indication of losses in highly permeable zones, and if drilling continues, a complete loss can occur [38].

2.4.2.4 Depleted Formations

Depleted formations, which have experienced fluid extraction, may exhibit subnormal pressures. In such cases, the mud weight required to control other exposed formations may be too high for the depleted formation, forcing mud into the low-pressure depleted zone. Stuck pipe incidents are common problems encountered in these situations [39].

2.4.2.5 Cavernous or Vugular zones

Cavernous formations, often composed of limestone, have large caverns or vugs formed by the continuous flow of water that dissolved part of the rock matrix through leaching. These void zones are often filled with oil. In these zones, lost circulation is sudden, complete, and particularly difficult to seal [40].

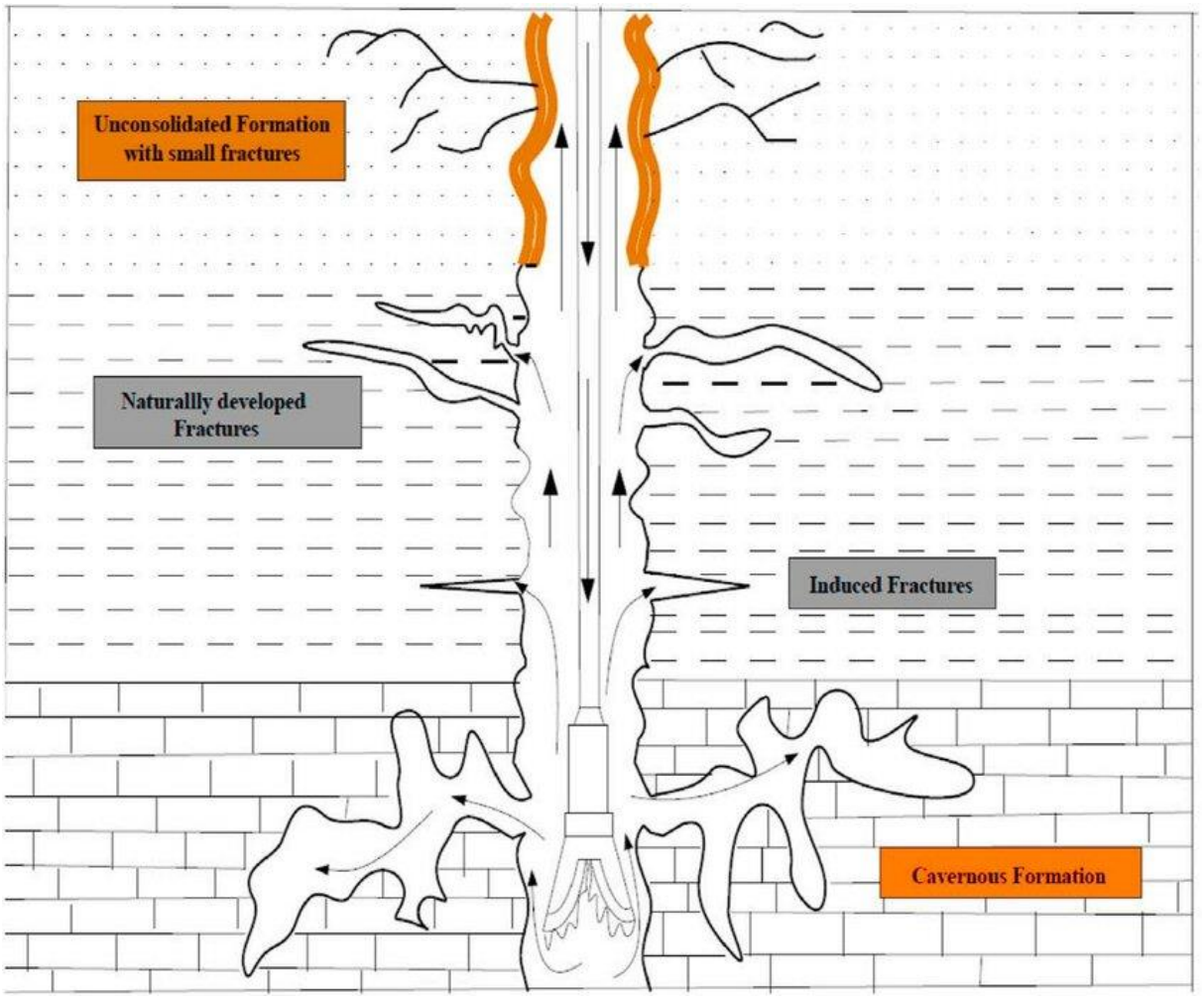

Figure 2.8 Various loss Circulation zones [41]

Having identified the potential loss zones, it is crucial to understand how circulation losses are classified. This knowledge is essential for making informed decisions regarding loss circulation management and determining appropriate actions to mitigate these losses.

2.5 Classification of Circulation Losses in Drilling

In drilling operations, lost circulation can be categorized into four primary types, and understanding the specific type and rate of losses is crucial for implementing the appropriate remedial measures [42]. The four types of lost circulation are as follows:

1. **Seepage Losses**: Seepage losses occur gradually, with a minimal volume of mud being lost into the formation. Although the impact on drilling operations is usually minimal and difficult to identify, seepage losses are commonly observed in highly permeable and porous zones such as gravel beds or shell beds. Due to the slow nature of these losses, they generally do not necessitate immediate well-control actions.

2. **Partial Losses**: Partial losses are more severe compared to seepage losses, where a significant volume of drilling fluid is lost into the formation, while some of it returns to the surface. However, the hydrostatic pressure is maintained, and a well control situation is not typically encountered. To address partial losses, drilling operations are temporarily halted to allow for remedial actions aimed at slowing down or curing the losses, ensuring that the drilling fluid can continue performing its intended functions effectively.
3. **Severe Mud Losses**: Severe mud losses involve the rapid and substantial loss of drilling fluid within short timeframes. This leads to a well control situation as the fluid level in the annulus decreases, resulting in reduced hydrostatic pressure and potential hole instability issues. Severe mud losses require immediate well control actions to restore the balance, typically involving the introduction of monitored volumes of lighter mud, water, or base oil into the annulus to refill the lost fluid.
4. **Total Lost Circulation**: When there is no mud returning to the surface, it is an indication of a complete or total lost circulation scenario. In such a situation, immediate and decisive well-control actions are required. In the event of total lost circulation, specific volumes of lighter mud, water, or base oil need to be used to refill the annulus to maintain well integrity and control wellbore pressure while closely monitoring the wellbore conditions. [43].

Table 1.1 presents the different classifications of circulation losses and their expected percentage loss rate.

Table 1.1: classification of severity losses and their prone formation types.

Severity of Loss	Percentage of Loss Rate (%)	Typical Formations
Seepage	<10 (bbl/hr)	Porous and permeable zones, shell beds/reef deposits.
Partial	10-50 (bbl/hr)	Unconsolidated sands and gravel
Severe	>50 (bbl/hr)	Large sections of unconsolidated sands/fractures
Total	100 (No returns)	Cavernous/large fractures

2.6 Lost Circulation Materials

When encountering lost circulation during drilling operations, the common approach to address this issue is through the use of lost circulation materials (LCM). LCMs are substances that can effectively seal openings in the formation to mitigate the loss of drilling fluids. There are two

primary mechanisms by which LCMs achieve this sealing effect: by forming a filter cake on the wall surfaces or by creating a bridge across fractures or openings within the formation [2]. The selection of an appropriate LCM depends on several key factors. Firstly, the formation lithology plays a crucial role in determining the LCM's compatibility and effectiveness. Different formations have varying characteristics, such as permeability and pore size distribution, which influence the choice of LCM. Secondly, the nature and severity of the loss zone also impact the selection process. The size and extent of the lost circulation zone, as well as the fluid pressure differentials involved, must be taken into account when determining the most suitable LCM.

Cost considerations also factor into the choice of LCM. The complexity of formation properties and loss characteristics can affect the overall cost of implementing LCM remediation. It is important to strike a balance between the effectiveness of the LCM and the associated costs to ensure a practical and efficient solution [44].

Although there is no universally accepted classification system for lost circulation materials (LCM), it is generally observed that the LCMs employed in drilling oil and gas wells can be categorized into three main groups:

1. **Fiber Lost Circulation Material**: Fibrous LCM consists of long, slender, and flexible materials available in various sizes and lengths. They are added to the drilling fluid to reduce losses and maintain circulation when facing lost circulation into fractures or highly permeable zones downhole. Examples of fiber LCM used in the oil industry include cedar fiber (wood fiber), sawdust (wood fiber), drilling paper (paper), magma fiber (mineral fiber), shredded cane stalks, and hair.
2. **Flaky Lost Circulation Material**: Flaky LCM is characterized by thin and flat shapes with large surface areas. Their purpose is to seal off mud loss zones in the well and prevent lost circulation by forming a mat over the pores in permeable formations. Flaky LCM should be insoluble and inert in the drilling mud system where they are used. Examples of flaky LCM include mica flakes, pieces of plastic, and cellophane.
3. **Granular Lost Circulation Material**: Granular LCM has a chunky shape and is available in a range of particle sizes. They are added to drilling fluids and pumped downhole to help prevent the loss of mud into fractures or highly permeable formations. Granular LCM should also be insoluble and inert in the drilling mud system. Examples

of granular LCM include nut shells, cotton hulls (coarse graphite), calcium carbonate (fine, medium & coarse), corncobs, wood, and Formica [42].

2.7 Lost Circulation Material Selection Approaches

To achieve an effective bridge at the fracture gate, it is crucial to select the appropriate particle size, shape, and concentration of LCM, along with using high-resilience LCM. The drilling fluid industry has developed theories to determine optimal particle sizes based on ideal packing theory and particle size distribution. Various approaches exist to optimize bridging blends and seal the formation surface based on the particle size distribution. Therefore, understanding the ideal particle size, shape, and concentration, along with choosing the right LCM, is essential to enhance drilling fluid performance and minimizing fluid losses [42].

2.7.1 Particle size distribution

Past studies from numerous authors have shown that carefully selecting the particle size of lost circulation materials is the main parameter for reducing filtrate loss when drilling through high permeability or fractured formations. Most of the common methods discussed below are generally built around the D50 or D90 values of the particles in the fluid as a relative size to the pore openings of the formation.[45]

2.7.2 Abrams Rule

Abrams (1977) introduced the 1/3 rule, which focuses on formulating minimally invading, non-damaging drill-in fluids. According to the rule, the mean particle size of the bridging agent should be equal to or slightly greater than 1/3 of the medium pore size of the target formation. Additionally, the solid volume concentration of drill-in fluids should be at least 5% (50 lb/bbl or 150 kg/m3). While the rule addresses the particle size that initiates a bridge, it does not provide the optimum size or consider the packing sequence for minimizing fluid invasion and optimizing sealing [46]

2.7.3 Ideal Packing Theory

Dr. Maurice E. "Dick" Matthews adopted the ideal packing theory from the paint industry and applied it to practical oilfield use. This theory proposes that the efficiency of solid particles in bridging and sealing fractures depends on their size and shape.

A key aspect of the theory is the importance of particle size distribution in achieving optimal packing. By selecting particles of different sizes, it becomes possible to fill void spaces and create a stable bridge, effectively preventing further fluid loss. It is crucial to know the pore size or fracture width to ensure ideal packing.

According to the ideal packing theory, ideal packing occurs when the percent of cumulative volume varies linearly with the square root of the particle size. This relationship helps in understanding and determining the appropriate particle sizes for effective bridging.

The theory also emphasizes the significance of particle shape. Non-spherical particles, such as elongated or irregular shapes, play a role in enhancing bridging efficiency. These particles can interlock with one another, creating a tighter seal and further improving the effectiveness of the bridging process [47]

2.7.4 Vickers Method

According to Vickers et al. (n.d.), the IPT (ideal packing theory) approach for lost circulation mitigation is limited to reservoirs with uniform pore throat distributions. As most reservoirs do not fit this description, an alternative model is required to achieve a more efficient bridge and reduce fluid loss into the reservoir.

Vickers proposed a particle selection method that aims to efficiently and rapidly bridge the largest, medium, and smaller pore size fractions. This method involves targeting five specific fractions, namely D90, D75, D50, D25, and D10. The Vickers criteria for particle selection are as follows [48]

- D90 = largest pore throat
- D75 < 2/3 of the largest pore throat
- D50 +/- 1/3 of the mean pore throat
- D25 1/7 of the mean pore throat
- D10 > smallest pore throat

2.7.5 Haliburton Method

The Halliburton method, developed by Don Whitfill, aims to prevent fracture propagation by isolating pressure communication between the mouth and tip of the fracture. This method utilizes the stress cage theory and selects a suitable particle size distribution (PSD) to create a bridge within the fracture, acting as a restrictive barrier to resist fluid flow.

The Halliburton method considers the relationship between particle size and filtrate volume. Smith et al. (1996) noted that a large mean particle size and a narrow size distribution would

reduce the number of particles passing through the slot disk, but it would result in a higher filtrate volume. On the other hand, increasing the concentration of fine particles can reduce the filtrate volume, but it would lead to more solid particles present in the filtrate.
To form an effective seal, the Halliburton method suggests that the PSD of the sealant material should be such that D90 equals the predicted fracture width, bridging at or just inside the point of fracture initiation [49] However, considering data uncertainty, the PSD is typically set with the D50 equal to the predicted fracture width. This approach ensures that both smaller and larger particles contribute to the formation of an effective seal.

2.8 Wellbore Strengthening Technique

The technique of wellbore strengthening has witnessed significant advancements over time, transitioning from simple plugging methods to a combination of plugging and prevention strategies. Wellbore strengthening revolves around enhancing the wellbore's ability to withstand the challenging conditions encountered during drilling operations, thereby improving overall well integrity. This technique involves increasing the breakdown pressure of the wellbore after treatment, aiming to fortify its stability and resistance to failure [50].

The advantages of implementing wellbore strengthening techniques extend beyond the scope of lost circulation alone. They include but are not limited to:

Wellbore strengthening techniques offer a multitude of advantages that extend beyond addressing lost circulation issues. These benefits encompass various aspects of drilling operations and include, but are not limited to:

- Access to additional reserves: By strengthening the wellbore, operators can access reservoir sections that were previously deemed unstable or prone to fluid losses. This enables the exploration and production of additional reserves that were otherwise challenging to reach.
- Reduced mud losses in deepwater drilling operations: Deepwater drilling environments pose unique challenges, including the risk of significant fluid losses. Wellbore strengthening techniques help minimize mud losses by enhancing the integrity of the wellbore, thereby reducing the associated operational and financial costs.

- Improved well control: Wellbore strengthening enhances the well's ability to withstand abnormal pressure conditions, improving well control during drilling operations. This increased stability minimizes the likelihood of wellbore collapse or uncontrolled fluid influx, contributing to safer and more efficient drilling processes.
- Elimination of casing strings: In certain cases, wellbore strengthening techniques can eliminate the need for additional casing strings. By fortifying the wellbore's stability, the reliance on additional casing can be reduced or eliminated, resulting in cost savings and streamlined drilling operations [1]

In the subsequent section, two common models used in wellbore strengthening treatments will be briefly discussed.

2.8.1 Stress Cage Model

The Stress Cage Model, developed by Aston et al during their work at BP, focuses on strengthening the wellbore while drilling. The model revolves around the concept of creating small fractures on the wellbore wall and keeping them open near the fracture openings using bridging particles. These bridging particles should possess low permeabilities to isolate pressure between the mouth and tip of the fracture, preventing fracture propagation. This technique generates increased hoop stress around the wellbore, referred to as the "stress cage" effect. To achieve this effect, suitable materials are added to the mud system to create a customized mud, as termed by Aston et al. The formula provided below can be used to calculate the pressure required to keep the fracture open.

$$\Delta_P = \frac{\pi}{8} * \frac{w}{R} * \frac{E}{(1-v^2)}$$

Where Δ_P is the excess pressure in the fracture (above the minimum principal in-situ stress, w is the fracture width, R is the fracture radius, E is the young modulus and v is the Poisson's ratio of the formation

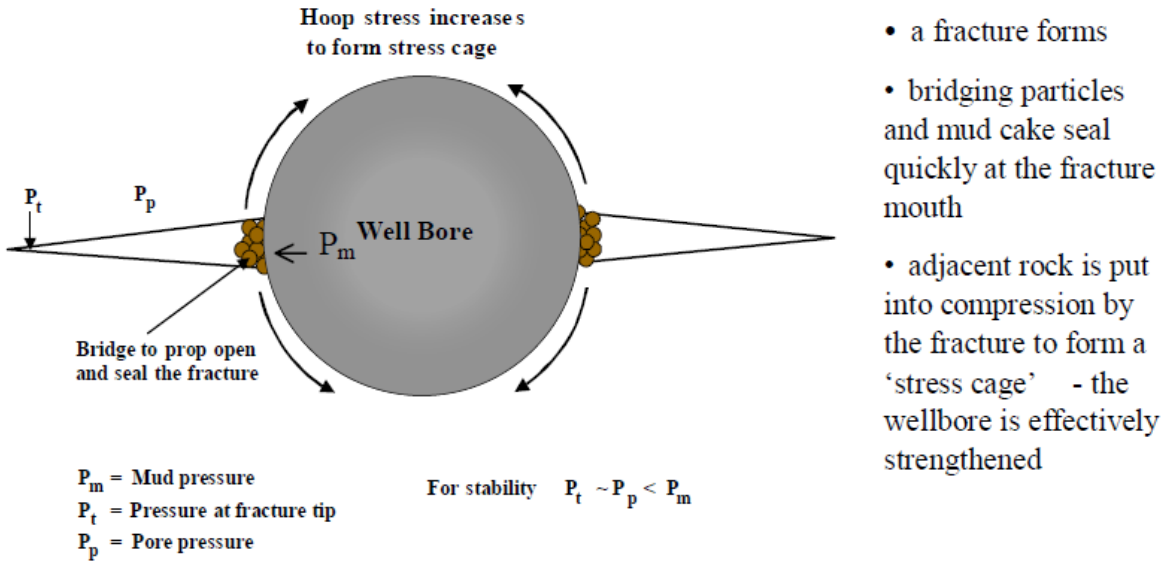

Figure 2.9: illustration of Stress Cage Effect [1]

Figure 2.9 provides a graphical illustration of the stress cage effect. The stress cage model was considered for two scenarios: permeable formations and non-permeable rocks with low permeability. In permeable formations, the stress cage effect is expected to be straightforward, as even if the bridging particle is not perfect, fluids passing through the bridge will leak away from the fracture into the formation, preventing pressure build-up and fracture propagation. Additionally, the pressure initially behind the bridge decreases when the fracture first forms, leading to increased effective stress across the fracture and subsequent closure behind the bridge. In the case of low-permeability rocks like shale, the bridging particle must have extremely low permeability to prevent pressure transfer into the fracture and fracture propagation. (for reference, the image is attached in the appendix)

Sensitivity studies conducted by [1] revealed the following observations:

- An effective wellbore strength of approximately 1000 psi can be achieved with fracture widths as small as 1 mm and fracture radii on the order of 1 meter.
- It is easier to reopen a fracture if the propped length is long and to achieve the same strength increase, a wider fracture width is required. Thus, a short fracture is preferable.
- Rocks with low Young's modulus necessitate larger fracture widths.
- The pressure required to keep the fracture open is not highly sensitive to Poisson's ratio.

In the experimental setup, the designer mud employed calcium carbonate and graphite blends as bridging particles. These materials had previously been used as Lost Circulation Materials (LCM) in BP's experiment, demonstrating favorable results as one of the most effective means to reduce mud losses into fractures. This influenced the selection of these materials. Test results indicated that the bridge remained intact under a maximum injection pressure of 1900 psi for a rock with a permeability of 160 millidarcy and a tapered fracture width from 1 mm to zero [1].

2.8.2 Fracture Closure Stress Model

The Fracture Closure Stress (FCS) operational practices were developed in the mid-1990s to prevent the problem of lost returns during drilling. The FCS model suggests that we can improve the integrity of fractures by widening them, which increases the force that keeps them closed. This force, called the closing stress, is made up of the compressive stress from the surrounding area and the stress near the wellbore. Instead of focusing on plugging the tip of the fracture, the key is to make the fracture wider [51]

The relationship between the width of the fracture and the closing stress can be explained using the linear elastic fracture mechanics model, which says that stress increases in proportion to the width. The compressibility of the rock is determined by its Modulus of Elasticity. It has been found that practices that maximize the overall width of the fracture tend to maximize the closing stress in areas where stress is concentrated. This has been supported by computer simulations and experiments in the lab. It's important to note that the final width of the fracture should be large enough to create a closing stress that exceeds the pressure of the drilling fluid. To achieve this, the treatment should maintain the isolation of the fracture tip as it widens and ensure a final width that can generate enough closing stress [51].

Using the FCS model with common Lost Circulation Materials (LCM) has achieved a success rate of nearly 100% in formations with good permeability. However, more progress is needed in formations with low or damaged permeability, and special products are being developed to improve success rates in these situations. The difficulty of the treatment depends on factors such as the permeability of the formation, the desired increase in closing stress, and the pressure difference between the drilling fluid and the small openings in the rock [51].

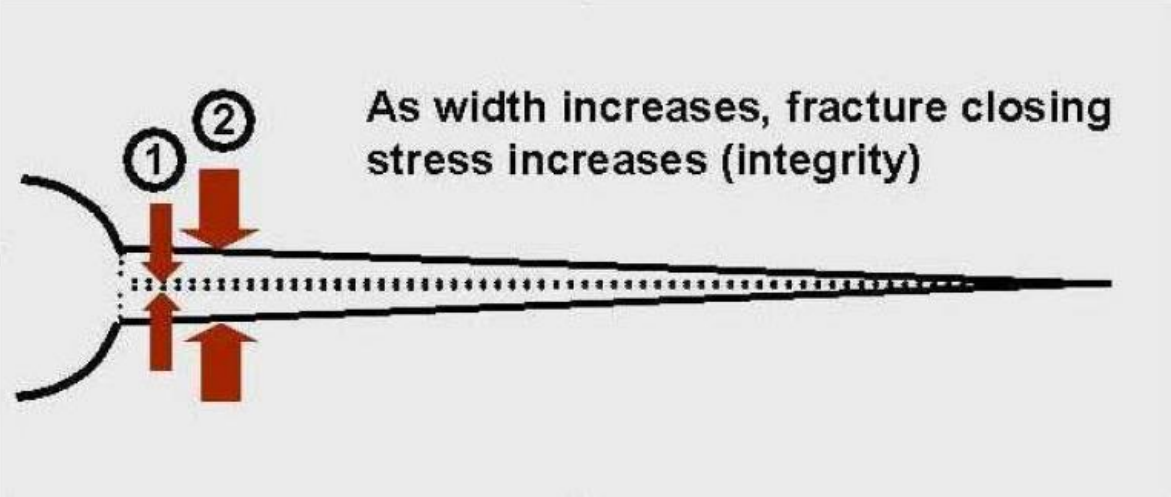

Figure 2.10: illustration of a fracture closure mechanism

Fracture closure stress is increased by widening the fracture to compress the adjacent rock. Closing stress determines opening pressure. Losses cannot occur if FCS > ECD.

2.9 Lost Circulation Management System

To manage lost circulation, industry professionals typically employ either preventive or remedial methods as illustrated in figure 2.11. Preventive measures focus on reducing the likelihood of fluid loss, such as optimizing drilling fluid properties and using specialized materials like LCMs to seal fractures. In severe cases, remedial action may be necessary, with the specific approach determined based on the severity of fluid loss rates in the formation [42]. Further explanation of the preventive and remedial methods is presented below.

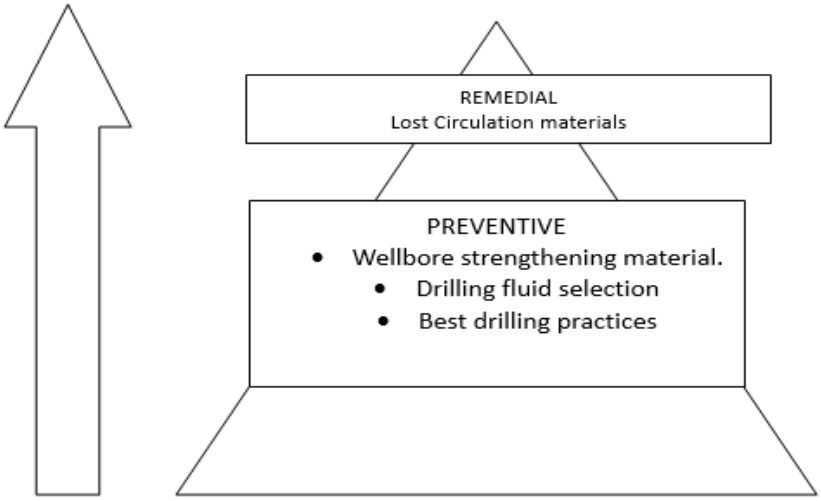

Figure 2.11: Lost Circulation Management Pyramid

2.9.1 Preventive Methods

Preventive methods focus on reducing the likelihood of lost circulation in the first place. One common preventive approach is to optimize the drilling fluid's properties, such as density, viscosity, and rheology, to match the formation being drilled. By tailoring the drilling fluid properties to the specific geological conditions, the risk of fracturing the formation and incurring lost circulation can be reduced.

Another preventive approach is to use Lost Circulation Materials (LCMs), which are specially designed additives that can help to seal fractures and prevent further fluid loss.

Other preventive measures include wellbore strengthening techniques, such as casing drilling, which reinforces the wellbore to reduce the risk of fractures and fluid loss [7]

2.9.2 Remedial Methods

Remedial methods are employed when lost circulation has already occurred. One common remedial approach is to use specialized LCMs designed to seal the fractures and prevent further fluid loss. These materials are typically added in larger quantities than preventive LCMs and can be combined with other additives to create a custom lost circulation treatment.

Another remedial technique is to inject cement into the wellbore to reinforce the formation and prevent further fluid loss. This approach is typically used in severe cases of lost circulation where traditional LCMs are not effective.

In some cases, remedial methods may involve temporarily stopping drilling operations to allow for specialized treatments to be injected into the wellbore.

By prioritizing lost circulation management and employing a proactive approach, drilling companies can increase operational efficiency, reduce costs, and improve safety on the rig [7].

2.9.3 Lost Circulation Treatment Decision Tree

When dealing with lost circulation during drilling operations in the oil and gas industry, a lost circulation treatment decision tree is commonly utilized to assist in selecting appropriate remedial actions. This approach has become a standard practice and its continuous refinement and application are crucial in addressing future lost circulation challenges.

The lost circulation treatment decision tree is a valuable tool for mitigating lost circulation in drilling operations. Offering a structured problem-solving approach, not only reduces costs and saves time but also enhances efficiency and minimizes formation damage.[2]

The field application of the lost circulation treatment decision tree involves a collaborative effort amongst drilling engineers, geologists, and mud engineers to diagnose and treat the issue. The decision tree provides a systematic framework for evaluating the problem and selecting the most suitable remedial actions. Furthermore, it enables real-time decision-making based on the ever-changing conditions in the wellbore.[52].

To further clarify the concept of the Lost circulation management tree, the following field cases are on Lost circulation and its management is reviewed in the subsequent section.

2.10 Field Case Study

2.10.1 Case 1: Enhancing Wellbore Stability/Wellbore Strengthening

The Cashiriari field in Peru faced challenges in maintaining wellbore stability due to natural and drilling-induced fractures, leading to lost circulation issues. The formations, Vivian and Chonta, comprised tectonically stressed sandstone and shale/sandstone bodies, necessitating a high inhibitive reservoir drilling fluid for hole stability. Minimizing mud losses during drilling, casing running, and cementing was crucial to reduce non-productive time.

To address these challenges, the Cashiriari field implemented wellbore strengthening techniques. The Hoop Stress Enhancement concept, known as the Stress Cage, was utilized to design the optimal Wellbore Strengthening Material (WSM) for the drilling campaign. The Stress Cage software package determined the suitable blend of WSM based on well design, rock properties, and in-situ stresses. Sized marble and graphite materials were recommended as WSM, continuously added at low concentrations during the drilling of the 12¼ in. x 8½ in. sections. The Hoop Stress Enhancement induced shallow fractures in the near-wellbore region, increasing the fracture resistance of the sandstone sections.

Furthermore, the Fracture Closure Stress (FCS) model was employed to increase tangential stress (hoop stress) around the wellbore, allowing for the use of higher mud weights without reaching the Fracture Breakdown Pressure. The FCS approach involved forcing high-fluid-loss pills into existing fractures to plug them and enhance the hoop stress. This technique could also be applied as a whole mud treatment by adjusting the drilling fluid properties to prevent lost circulation.

The implementation of WSM and FCS in the Cashiriari field successfully reduced lost circulation and improved fracture resistance, enabling faster and deeper drilling in subsequent wells. Valuable lessons learned from field applications were continuously utilized to optimize the wellbore stability techniques [53].

2.10.2 Case 2: Mitigating Lost Circulation in the Dammam Formation

Hameedi et al (2018) [2] conducted a comprehensive study in 2018, focusing on lost circulation challenges encountered in the Dammam formation of the Rumaila field in Iraq. Their research involved a statistical analysis and sensitivity study of over 300 wells drilled in the formation to identify the key parameters influencing mud loss volumes. Based on their findings, the authors developed three mathematical models to estimate mud losses, equivalent circulation density (ECD), and rate of penetration (ROP). These models offer valuable tools for predicting expected mud losses and establishing drilling parameters to minimize losses during drilling operations.

Furthermore, the study encompassed a thorough examination of lost circulation treatments specifically designed for the Dammam formation, encompassing both preventive and remedial solutions. To provide a concise overview of the treatment options, the authors presented a flowchart that outlines strategies for partial, severe, and complete losses. The study's insights serve as a valuable resource for drilling engineers and professionals operating in the Dammam formation or similar geological formations, offering guidance in effectively managing lost circulation challenges [2]

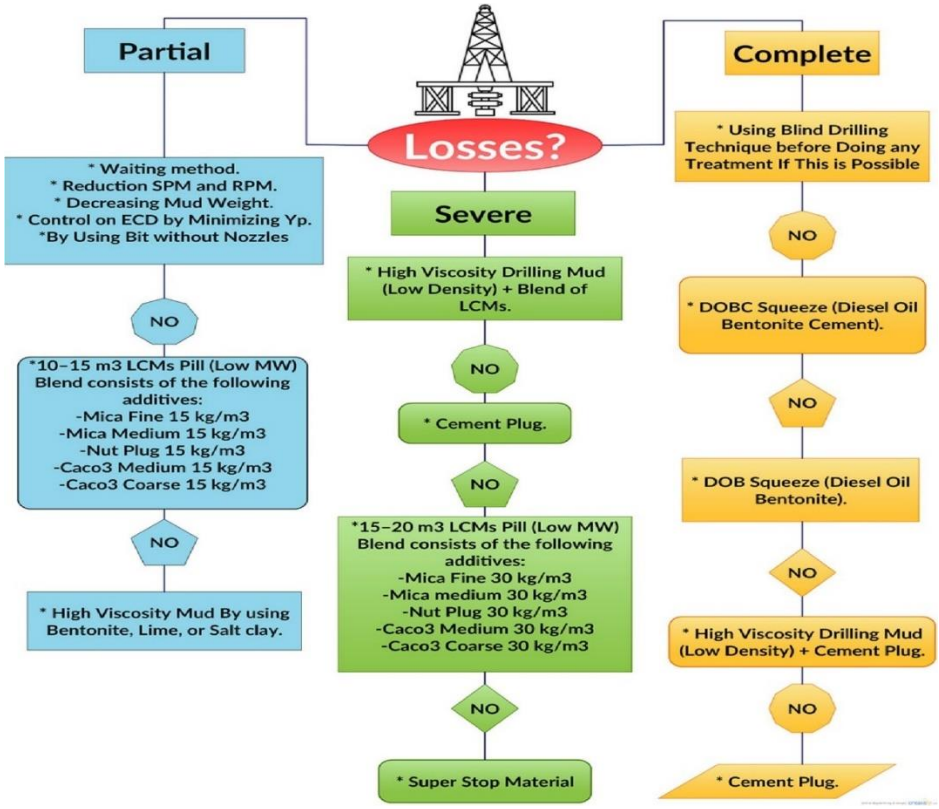

Figure 2.11: Flowchart for Lost Circulation Management [2]

2.10.3 Case 3: Lost Circulation Planning for Deepwater Sub-salt Wells

The planning phase for a deepwater, sub-salt well in the Gulf of Mexico incorporated the Lost Circulation Assessment Process (LCAP) due to anticipated lost circulation challenges based on previous offset wells. The study focused on three intervals: 14 ½-in, 12 ¼-in, and 9 7/8-in, characterized by Miocene lithology comprising shale, sandstone, and a transition zone with potential limestone stringers. The immediate thief zone below the salt formation was expected to be a highly fractured shale rubble zone.

While the fracture gradient in the rubble zone was of less relevance, variations in the estimated range of 14.5 - 15.0 lb/gal mud weight equivalent were anticipated. To address potential lost circulation zones, a development team was assembled, relevant data was gathered, and an LCAP document was generated. The primary zones of potential losses were identified as induced fractures in shale, porous sandstone, induced fractures in sandstone, and natural fractures in sandstone. Considering the typical drilling scenario of using synthetic-based mud (SBM) in wells of this nature, a suitable formulation for mitigating seepage losses involved a blend of granular calcium carbonate and synthetic graphite. Optional treatment approaches

were considered, ranging from conventional to specialized techniques, including pre-treating the mud system with CaCO3 and synthetic graphite, incorporating fiber-based particulate lost circulation material (LCM) as the system passed through the seepage loss zone, pumping synthetic graphite sweeps at specified intervals, and utilizing a sequence of blended LCM pills of varying densities.

To guide decision-making for lost circulation issues in this deepwater prospect, a series of lost circulation decision trees were developed. These decision trees provided a systematic approach to address the different lost circulation scenarios encountered during drilling operations [3].

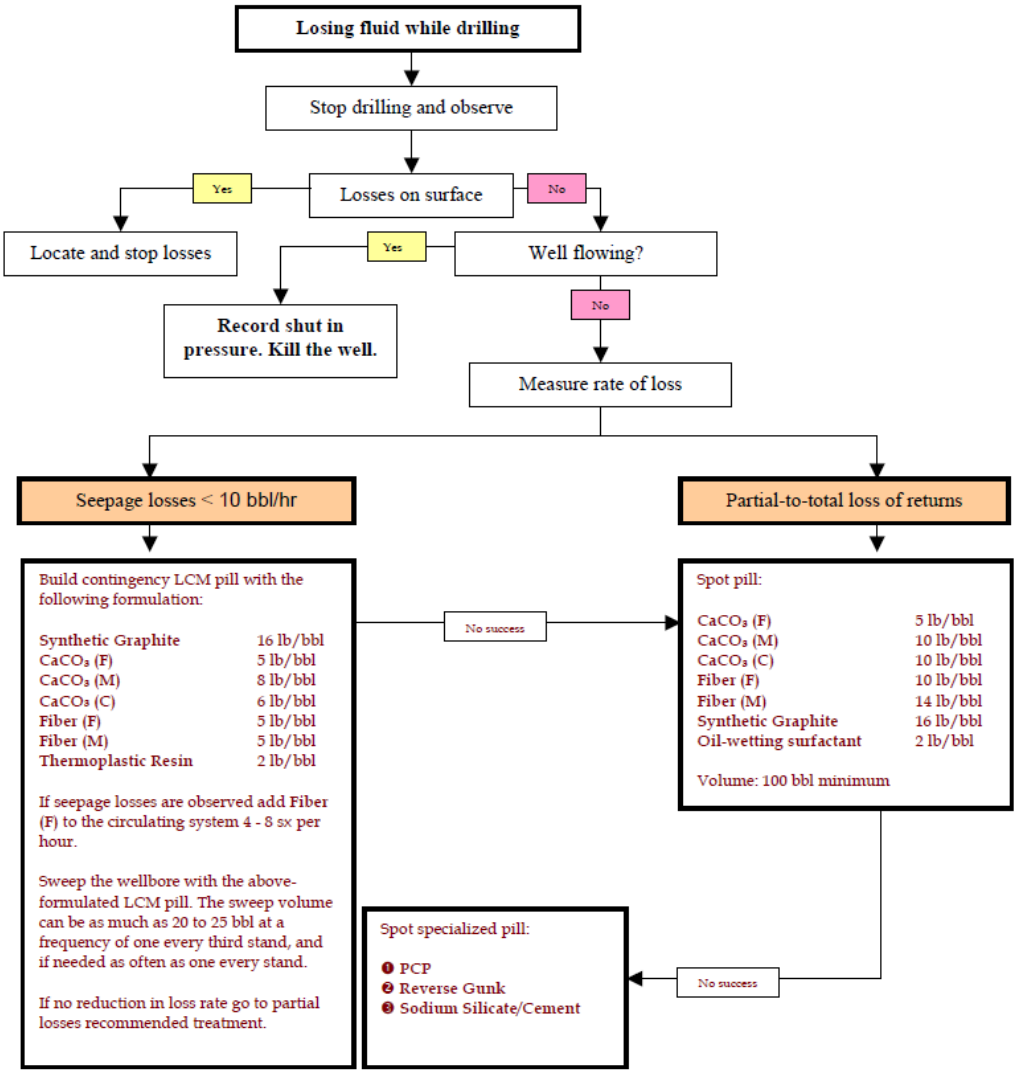

Figure 2.12: Lost Circulation Management Decision tree for a Deepsea Prospect [3]

3 Experimental Work

The primary objective of experimental work is to observe and analyze natural or engineered systems in a controlled environment, to obtain significant findings, and draw insightful conclusions based on the data obtained. In the following sections, a concise overview of the materials and methods used to obtain data and results in this study is presented. The figure below is a visual representation of the study plan for the experimental work.

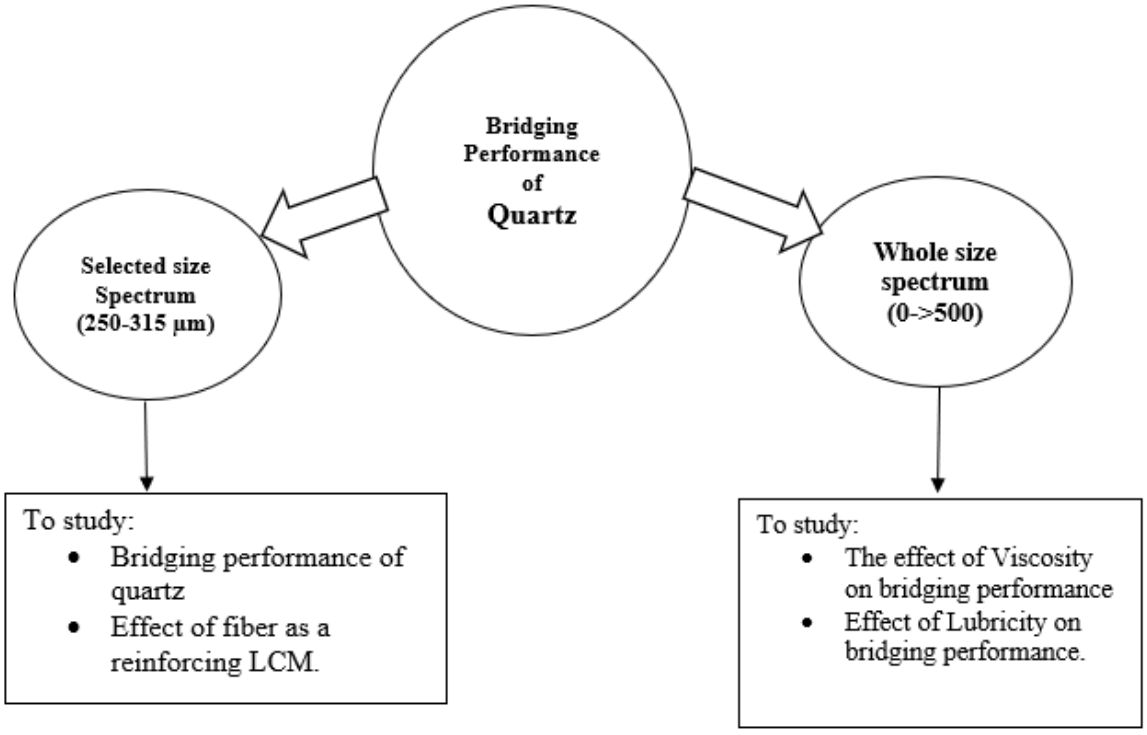

Figure 3.1: Experimental Study Plan

1. Investigation of Quartz Performance as an LCM Particle in Bentonite-Based Drilling Fluids: This experiment focuses on assessing the stability of Quartz particles when incorporated into Bentonite-based drilling fluids. The objective is to examine how Quartz performs as an LCM in this particular fluid system.
2. Correlation Analysis between Fluid Rheological Parameters and Bridging Pressure in Water-Based Mud: Here, the objective is to explore the possibility of establishing a correlation between the bridging pressure exhibited by the fluid and its rheological parameters.

3. Evaluation of Fiber Additives for Particle Stability Enhancement: The impact of fiber additives on particle stability within the fluid system is investigated in this experiment. The objective is to analyze how the addition of fiber enhances the stability of LCM particles and their performance.
4. Assessment of Particle Size Distribution (PSD) (Quartz and Fiber) on Bridge Stability: This experiment seeks to understand the influence of particle size, particularly with respect to fracture width, on bridge stability. By examining the performance of LCM particles (Quartz) and fibers in terms of PSD, the study aims to gain insights into the relationship between particle size and bridge stability.
5. Investigation of the impact of lubricity on bridge stability is explored by evaluating the performance of Quartz particles as LCMs in two fluid systems of varying lubricity. The objective is to analyze how lubricity influences the stability of the bridge formed by LCM Quartz particles.

3.1 Materials

3.1.1 Bentonite

Bentonite is a type of clay mineral that is widely used in the oil and gas industry as a crucial component of drilling fluids. Its exceptional properties and characteristics make it a highly desirable material for this application. One of the primary roles of bentonite in drilling fluids is to act as a viscosifier, which helps to increase the viscosity of the fluid and prevent fluid loss from the borehole.

The high surface area of bentonite is one of the reasons why it is widely used in the oil industry. This characteristic allows it to have a large number of reactive sites that enable it to interact with other chemicals and minerals present in the drilling fluid. Additionally, bentonite has a cation exchange capacity, which allows it to absorb and exchange ions with its surroundings. This unique property helps to maintain the stability of the drilling fluid by preventing unwanted chemical reactions.

Another remarkable feature of bentonite is its colloidal nature. This property enables it to form stable suspensions in water, which is essential for maintaining the viscosity of the drilling fluid.

The colloidal property of bentonite also helps to enhance the filter-cake formation, which is important for preventing the loss of drilling fluid and minimizing formation damage [54].

3.1.2 Barite

The chemical and physical properties of barite make it an ideal material for use in drilling fluids. Barite is a mineral that is commonly used in the oil and gas industry as a weighting agent in drilling fluids. Its primary function is to increase the density of the fluid, which helps to control the pressure in the wellbore and prevent blowouts.

One of the most important properties of barite is its high specific gravity, which is typically around 4.5 g/cm^3. This property allows it to provide the necessary weight to the drilling fluid without adding excessive volume, making it more efficient and cost-effective compared to other weighting agents. Additionally, barite is chemically inert, which means that it does not react with other chemicals in the drilling fluid or with the surrounding formation.[55]

Barite is also easy to process and transport, making it a practical choice for drilling operations. It is available in a range of particle sizes, from fine powders to coarse granules, which allows for customization based on the specific needs of the wellbore. Furthermore, barite has a low abrasion rate, which helps to minimize damage to the drilling equipment and the formation.[56]

3.1.3 Soda Ash

Soda ash, or sodium carbonate, is a chemical compound that has been utilized in the oil and gas industry as a pH regulator in drilling fluids. It is highly effective in controlling the alkalinity of drilling fluids, which helps prevent corrosion of the drilling equipment and minimizes damage to the formation. Soda ash is highly soluble in water and can easily disperse in drilling fluids, which makes it easy to handle and apply. Its non-toxic and environmentally friendly nature makes it a safe choice for use in drilling operations, which is an important consideration given the growing focus on environmental sustainability in the oil and gas industry.

Another critical property of soda ash is its ability to react with acidic substances, which enables it to neutralize and balance the pH of drilling fluids. This feature is particularly important in high-temperature and high-pressure environments where drilling fluids can become acidic and

corrosive. By regulating the pH of drilling fluids, soda ash can help maintain the integrity of the wellbore and maximize drilling efficiency.[57]

3.1.4 Carbopol

Carbopol is a synthetic polymer that is widely used in the oil and gas industry as a rheology modifier to increase the viscosity of drilling fluids, improve hole cleaning, and enhance suspension properties. Its chemical and physical properties make it a suitable choice for this application. Carbopol is thermally stable and resistant to degradation, which makes it suitable for use in high-temperature and high-pressure environments. It is also tolerant of salt and other contaminants, making it appropriate for use in high-salinity conditions. Moreover, Carbopol is pH-sensitive, meaning that its viscosity can be easily controlled by adjusting the pH of the drilling fluid. In addition, Carbopol is easy to handle and disperse in water, making it a practical choice for drilling operations. However, care must be taken to avoid overusing Carbopol, which can lead to excessive thickening and increased viscosity of the fluid system [58].

3.1.5 Poly-Pac

Poly-Pac is commonly used in water-based muds to control fluid loss. It can work effectively in a wide range of conditions including varying salinity, hardness, and pH levels. When added to drilling fluids, it forms a thin, low-permeability filter cake that minimizes differential sticking and invasion of filtrate and mud solids into permeable formations, which can lead to hole shrinkage and collapse. Poly-Pac is also effective in encapsulating exposed shales and drill cuttings, forming a protective polymer envelope that inhibits the dispersion of shale cuttings and restricts fluid interactions with exposed shales. It has excellent environmental acceptability and can enhance viscosity and control fluid loss even at low concentrations [59].

3.1.6 Saraline G100

Saraline G100, developed and manufactured by Shell, a renowned leader in the oil industry, is a hydrocarbon fluid derived from natural gas feedstock through Shell's proprietary catalyst technology. Primarily used as a drilling fluid, particularly in oil-based mud applications, Saraline G100 exhibits lubricity effects and serves as a lubricant in this thesis to enhance the investigation of lubricity effects in synthesized fluids.

In addition to its lubricity-altering properties, Saraline G100 offers the advantage of not being classified as a physical or environmental hazard. Extensive evaluations have determined its non-hazardous nature in terms of physical risks and environmental impacts, in compliance with

the European Union Classification and Labelling and Packaging criteria (CLP) for chemicals. However, it is important to exercise caution and avoid ingestion [60].

3.1.7 Graphite

Graphite is a naturally occurring form of carbon that is commonly used in the oil and gas industry as an additive in drilling fluids. Its use as a lubricant and friction reducer helps to reduce wear and tear on drilling equipment, improving operational efficiency and reducing costs. Graphite has several desirable chemical and physical properties that make it well-suited for this application. It is highly stable and inert, non-toxic, and has high thermal stability, which allows it to maintain its lubricating properties under high temperatures and high-pressure conditions. Additionally, graphite has a low coefficient of friction and is easily dispersed in drilling fluids, making it a practical choice for drilling operations [61].

3.1.8 Lost Circulation Materials

3.1.8.1 Quartz

Quartz is a mineral consisting of silicon and oxygen atoms that are widely used as a lost circulation material (LCM) in the oil industry. Its suitability as an LCM is due to its physical and chemical properties.

Quartz's high hardness, chemical inertness, and compatibility with most drilling fluids make it an excellent choice for use as an LCM. It is also available in various particle sizes, which enables it to effectively seal both large and small fractures in the formation. Additionally, it has high thermal stability, making it resistant to the high temperatures experienced during drilling.

Overall, the unique properties of quartz, coupled with its widespread availability, make it a popular choice as an LCM in the oil industry.

3.1.8.2 Particle size Distribution

The particle size distribution (PSD) analysis was conducted to determine the range of particle sizes in the Quartz sample, which would help in selecting appropriate slot sizes (fracture wings)

for the experiment. However, it was not feasible to perform a PSD for the wood fibers used because they are too light to pass through the sieve holes.

The PSD curve shown below indicates that the Quartz particles have a D50 value of between 315-355, which means that half of the particles fall within this range.

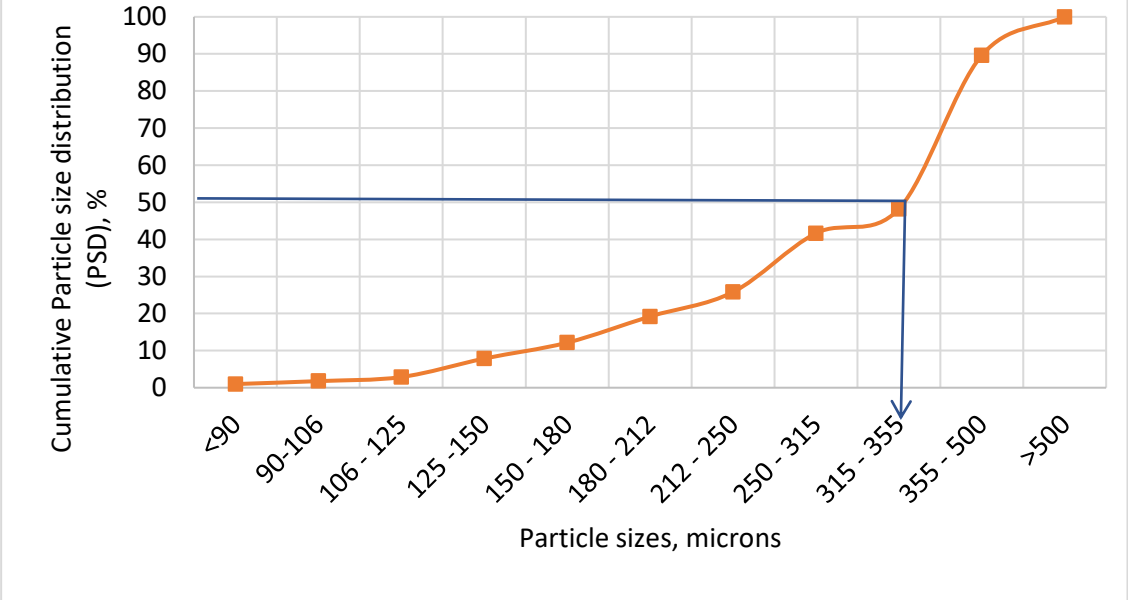

Figure 3.2: Particle Size Distribution of Quartz particles used

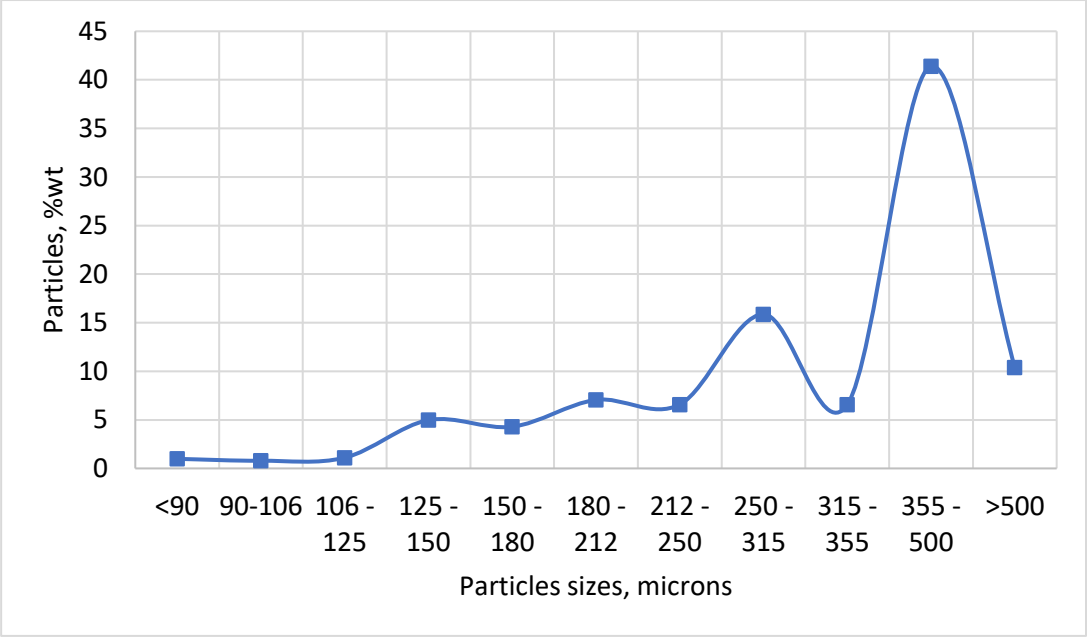

Figure 3.3: Particle weight Percent of Quartz particles used.

3.1.8.3 Wood Fiber

Wood fiber is a natural product derived from wood and is commonly used as a lost circulation material (LCM) in the oil industry. Wood fiber is desirable as a lost circulation particle due to its low density, low cost, and biodegradability. It is also available in a range of sizes, which allows it to effectively seal both large and small fractures in the formation. As lost circulation material, wood fibers are added to the drilling mud, which is then pumped into the wellbore. When the mud containing wood fibers reaches the fracture or fissure, the wood fibers are forced into the openings, where they can form a mat or network of fibers that effectively seal the gaps or provide support for other bridging particles. The wood fibers can also swell when they come into contact with water, which further enhances their sealing ability by creating a denser and more solid mass.

Figure 3.4: Wood fiber (left), shredded wood fiber (right)

3.2 Experimental Equipment

3.2.1 Viscometer

In the oil industry, the Fann 35 viscometer is a commonly used instrument in the lab for measuring the rheological properties of fluids. It is a rotational viscometer that measures the torque required to rotate a spindle at a constant speed in a fluid sample.

To test the viscosity of the drilling fluids prepared, a sample of the fluid is prepared and placed in the measuring cup. The spindle is then lowered into the fluid and rotated at a constant speed

while the torque required to maintain the rotation is measured. The viscosity of the fluid is then calculated using the Fann 35 equation, which takes into account the spindle speed, the spindle geometry, and the torque reading.

The viscometer is a reliable and accurate instrument for measuring the rheological properties of fluids in the lab and is widely used in the oil and gas industry [62].

Figure 3.5: Fann 35 viscometer

3.2.2 Tribometer

The figure shown below is a photograph of a rotating ball tribometer used in this experiment to test the frictional properties of the prepared fluids. The instrument consists of a rotating ball that applies a controlled load on the fluid sample while measuring the frictional forces acting on it.

The procedures for performing this test are outlined below:

- A sample of the fluid under test is placed in a test cell, which is usually a small container with a flat surface. A ball of a known diameter, usually made of a hard material such as steel or diamond, is mounted on a spindle.
- The spindle is lowered onto the fluid surface, applying a controlled load on the ball.
- The ball is rotated against the fluid surface at a constant speed. The rotation speed can be adjusted to simulate different sliding or rolling speeds.

- A force sensor is used to measure the friction force between the ball and the fluid surface. The friction force is a function of the load, speed, and fluid properties.
- The result is analyzed and the test is repeated before the average of the two results is taken as the coefficient of friction.

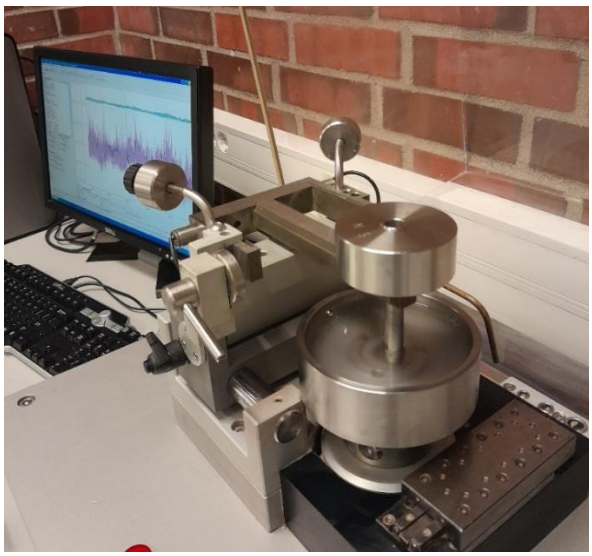

Figure 3.6: Rotating ball tribometer

3.2.3 Sieve Analyzer

A sieve shaker, which is a laboratory instrument utilized for the particle size analysis of solids, powders, and granules, involves the usage of a set of sieves with varying mesh sizes arranged in a stack, where mechanical vibrations are applied to separate particles based on their size. In this study, the sieve shaker was employed to determine the particle size distribution of Quartz particles. Specifically, a known concentration of Quartz was weighed and carefully placed on the top sieve of the stack that was composed of sieves with different mesh sizes arranged in descending order. The machine was programmed to set the testing parameters, such as the duration and intensity of the shaking, accordingly. Subsequently, the instrument applied mechanical vibrations to the sieves, inducing the particles to move and settle in the mesh openings based on their size, while adjusting the vibrations to achieve the targeted degree of separation. Following the completion of the shaking process, the sieves were removed from the stack, and the particles remaining on each sieve were weighed. Finally, the weight of each fraction was utilized to calculate the particle size distribution.

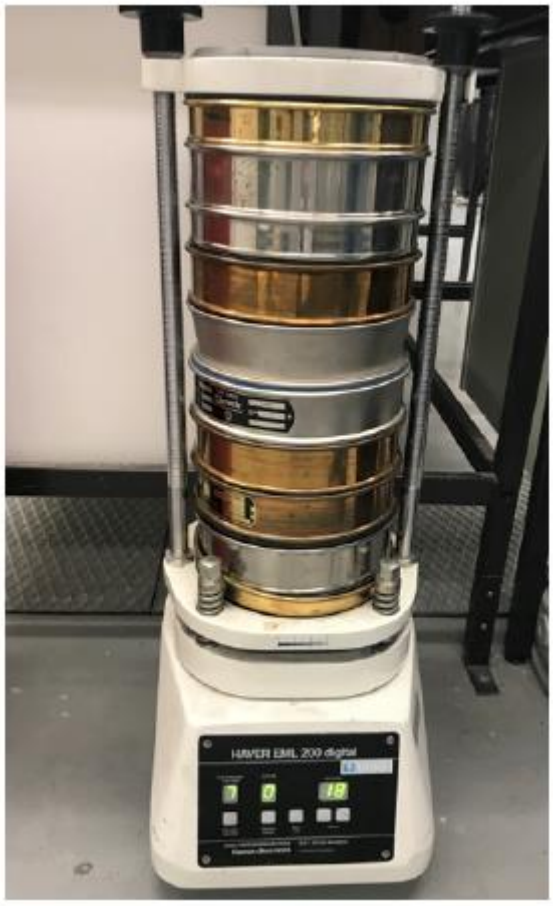

Figure 3.7: Sieve Shaker

3.2.4 Lost Circulation Static Bridging Apparatus

The experimental setup for the static bridging test at the University of Stavanger comprises a cylindrical drilling fluid holder (5) with dimensions of 35 mm (inner diameter) and 64 mm (outer diameter) and 150 mm long. The cylinder contains a detachable slot that sits at the bottom of the cylinder and simulates a fractured wing. The slot has a depth of 10 mm and a length of 24.4 mm.

To conduct the test, a blend of drilling fluid and LCM is poured into the cylindrical fluid holder, which forms a mud cake (4) at the gate of the slot (7), as shown in Figure 12. Ionized water is then pumped into the slot to fill up the space behind the drilling fluid mixture in the cylinder, while the valve (9) is left open for overflow.

The pressure response on the mud cake is recorded using PC-control (1) and the Gilson pump (2) applies the pressure. Once the void space in the cylinder has been filled up, the top valve is

closed (3) and the valve (6) at the bottom of the cylinder is opened to allow for fluid losses through the slot while the test is ongoing. Care is taken to start by pouring the mixed drilling fluid and LCM particles into the cylinder (5) to maintain a dispersed fluid system and avoid having the heavier LCM particles settle at the slot gate early in the test. This test method is used to investigate the effectiveness of LCMs in preventing fluid losses caused by fractures.

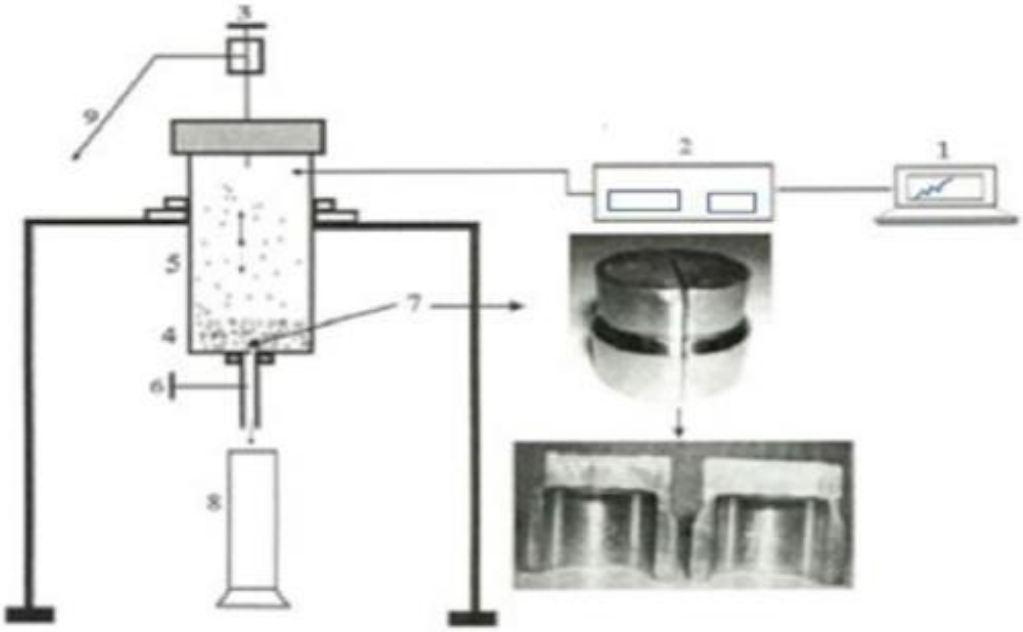

Figure 3.8: Schematic Diagram of the Static bridging test Experimental setup

3.3 Drilling Fluid Synthesis

In this section, we present a description of two distinct types of fluids utilized in this study. The first fluid system referred to as drilling fluid 1, was employed to examine the bridging performance of quartz. On the other hand, the second fluid system, called drilling fluid 2, represents a less realistic drilling mud used to investigate the influence of viscosity and lubricity. A detailed description of the fluids is presented in subsequent sections below.

3.3.1 Drilling Fluid 1

The fluid system was prepared in 4 batches due to limited capacity and to ensure effective mixing, each batch was prepared using the additives listed in Table 3.1. The preparation followed the procedures outlined in [63].

Table 3.1: Drilling fluid 1 additive and mixing process

Additives	Quantity	Mixing Method	Mixing time
Barite	150 (g)	Mixed under high speed	3 (mins)
Bentonite	10 (g)	Mixed under low speed while pouring into the mixing cup. Then later stirred at high speed.	10 (min)
Carbopol	0.14 (g)	Stirred under medium speed	2 (mins)
Soda ash	3.2 (g)	Mixed under medium speed	5 (min)
Tap water (H2O)	350 (g)		
Poly-pac	0.5 (g)	Mixed at high speed	2 (min)
Pac	0.25 (g)	Mixed at high speed	2 (min)

A digital scale was used to measure the quantities of the additives, which were then mixed and stirred using the Hamilton mixer. While other additives readily dissolved in water, bentonite required rigorous mechanical stirring to ensure even mixing.

To prevent the flocculation of bentonite particles, it was gradually added to the fluid mixture while being stirred under the mixer. The remaining bentonite bubbles in the mixture were smashed on the wall of the mixing cup and later stirred under the mixer to achieve a uniform solution.

After the mixing process, the fluid was allowed to blend evenly for 24 hours, before measuring the rheological properties using the viscometer, the measurements are presented in Table 3.2.

Table 3.2: Drilling Fluid 1 Rheological Measurement

RPM	Drilling fluid 1 (Reading)
600	41.2
300	29
200	23
100	17.5
60	15.5
30	14
6	12
3	11.5

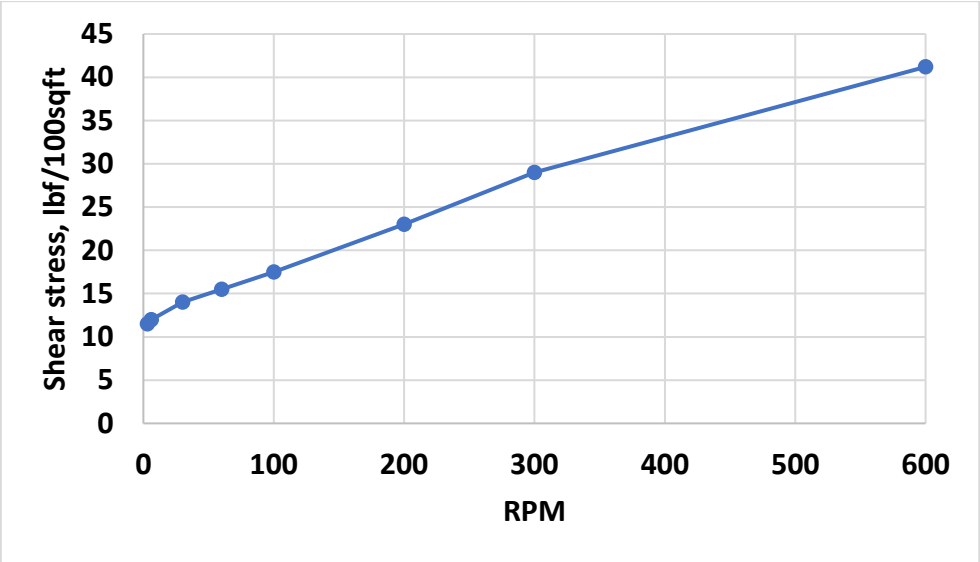

Figure 3.9: Rheology Measurement for Drilling Fluid 1

3.3.2 Drilling Fluid 2

This drilling fluid was intentionally designed to be less realistic; the objective was to create a controlled rheological profile with minimal/no interference from other additives. The primary constituents of the fluid were water (H2O) and Bentonite, with varying concentrations used to exert precise control over the fluid's viscosity. This approach enabled a more thorough investigation into the effects of viscosity and Lubricity on the fluid's performance.

3.3.2.1 Fluid for Viscosity Investigation

To achieve the desired goal for the viscosity investigation, drilling fluid 2 was prepared in three distinct types, labeled A, B, and C, with each type containing increasing amounts of Bentonite. For each type, a specific quantity of Bentonite (12.5g, 15g, and 20g) was thoroughly mixed with 350 mL of water (H2O) in a single batch. To ensure reproducibility, four batches were prepared for each fluid type and the mixing procedures and quantities are listed in Table 3.3.

Table 3.3: Drilling fluid 2 additives and formulation

Fluid	Additives	Mixing time	Mixing method
Type A	350 (ml) water + 12.5 (g) Bentonite	10min	Stirring
Type B	350 (ml) water + 15 (g) Bentonite	10 min	Stirring
Type C	350 (ml) water + 20 (g) Bentonite	10 min	stirring

Upon initial observation, type C appeared to exhibit higher viscosity compared to the other samples. To mitigate this issue, a solution of 0.3 g of Lignosulfonate in 50 g of water was mixed into the entire mixture (4 batches) of type C fluid to reduce its viscosity to levels that were more consistent with the other samples.

The fluid mixture settled for 24 hours, and viscometer responses of the drilling were measured and presented in the subsequent tables.

Table 3.4: ***Drilling fluid 2 viscometer dial reading measurement***

RPM	Type A	Type B	Type C
600	17	24.5	31
300	13	18.5	24.5
200	11.5	16.5	21.5
100	9	14	18.5
60	8	12.5	17.5
30	7.5	11.5	16
6	6.5	9.5	13.5
3	6	9	13

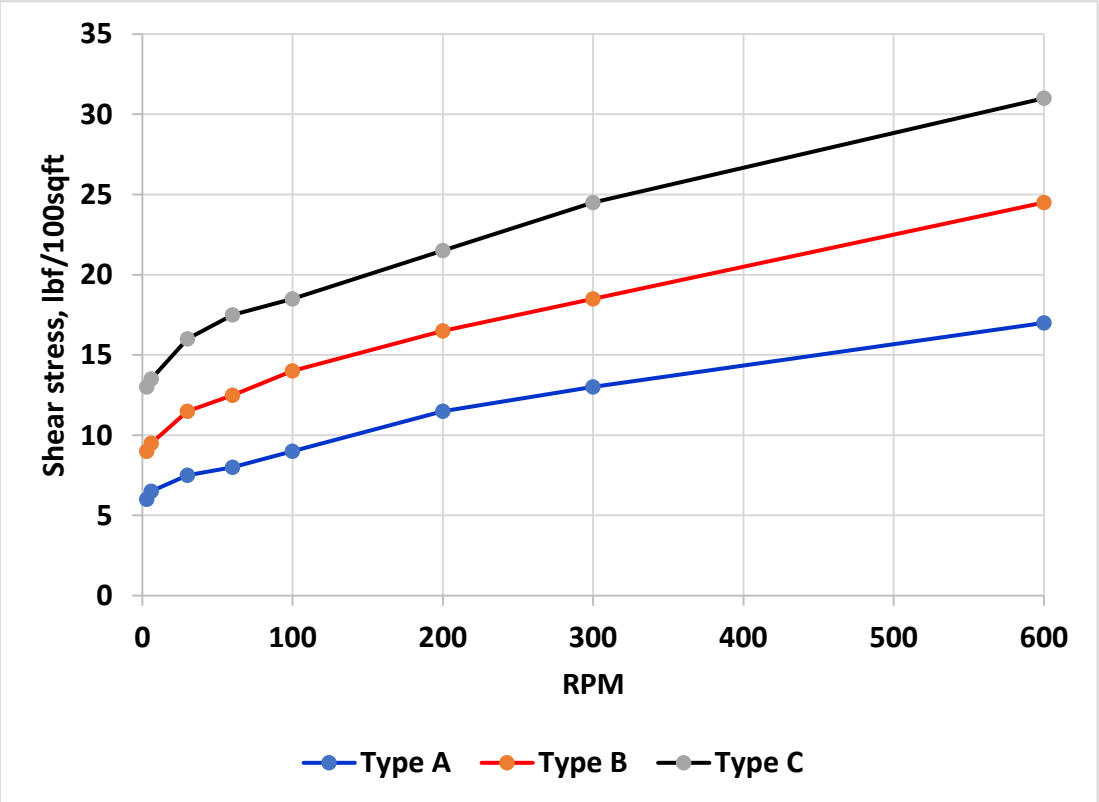

Figure 3.10: Rheology Measurement for Drilling Fluid 2

Table 3.5: ***Calculated Rheological Parameters of Drilling Fluid 2.***

Rheology Parameter	Type A	Type B	Type C
Plastic viscosity (PV)	4	6	6.5
Yield Strength (YS)	9	12.5	18
Low shear yield stress (LSYS)	5.5	8.5	12.5
n-parameter (n)	0.3868	0.4050	0.3393
k-parameter (k)	1.1650	1.4798	2.9528

3.3.2.2 Fluid for Lubricity investigation

For the lubricity investigation, drilling fluid 2 containing 15 grams bent was chosen as the reference fluid, this was prepared in 4 batches, each batch was prepared by mixing 15g of bentonite with 350g of water. The goal of the fluid synthesis for this test was to prepare a fluid system that didn't show significant deviation in rheological parameters, making it possible to vary only the coefficient of friction (COF) of the fluid samples and investigate the effect of lubricity on particle bridging performance. This was attained by adding lubricants to the fluid system to alter the COF of the fluid system as shown in Table 3.6.

Table 3.6: Additives and Formulation of drilling fluid for lubricity investigation

Fluid Type	Additives
Reference fluid	15 g Bentonite + 350 g H2O
Base Oil Lube	Reference fluid + 1.5 g base Oil
Graphite base Oil Lube	Reference fluid + 1.5 g of Graphite-treated base oil lube (5% graphite)

The rheological measurement of the 3 fluid types was measured using a viscometer, the results are shown in Table 3.7, and the calculated rheological parameters are in Table 3.8.

Table 3.7: Viscometer readings for Lubricity test drilling fluids

RPM	Reference fluid	Ref + 1.5g Base Oil lube	Ref + 1.5g of 5% Baseoil-graphite lube
600	24.5	24.5	25.5
300	20.5	20.5	21
200	18.5	19	19
100	16.8	16.5	17
60	15	15.5	16
30	14	14.5	14.5
6	13.5	13.5	13.5
3	13	13	13

Table 3.8: Calculated Rheological values for Lubricity test drilling fluids.

Fluid	PV	YS	LSYS	n	k
Reference fluid	4	16.5	12.5	0.25700858	4.1273039
Ref + 1.5g Base Oil lube	4	16.5	12.5	0.25700858	4.1273039
Ref + 1.5g of 5% Baseoil-graphite lube	4.5	16.5	12.5	0.25700858	4.1273039

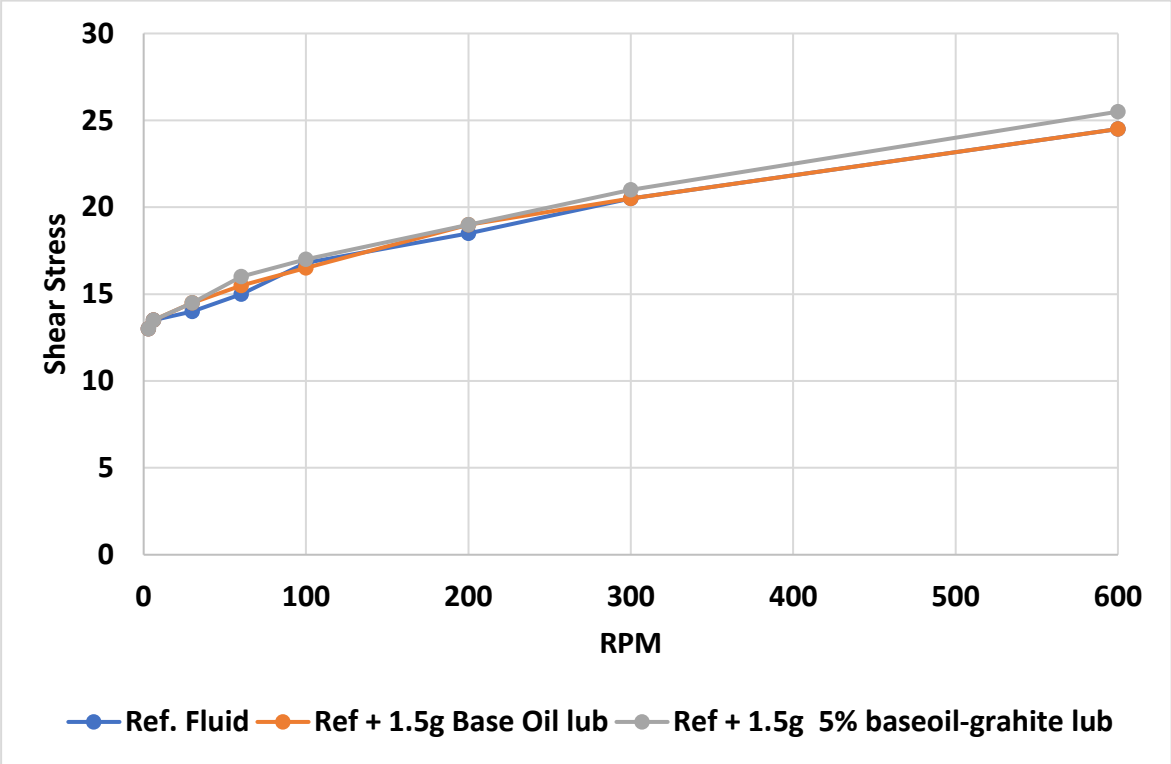

Figure 3.11: Rheology measurement for lubricity fluids.

As can be observed from the rheology measurement plot, the 3 fluid systems prepared for this testing show similar rheological properties, that is, the addition of the lubricants did not alter the rheological properties of the fluid. This observation is particularly important as it ensures that the only changing variable would be the Coefficient of friction (COF), enabling a thorough investigation of the effect of lubricity without the contribution of viscosity.

The coefficient of friction was measured for the fluids with lubricants and the result is presented in the table below.

Table 3.9: Friction test Results for lubricity investigation

Fluid	Base Oil Lube	Graphite base Oil Lube
Friction Test 1	0.368	0.281
Friction Test 2	0.396	0.280
Average	0.382	0.280

4 Results and discussion

4.1 Effect of Quartz -Selected particle size spectrum

The findings are organized into two distinct sections. The initial section delves into an examination of quartz performance in a single-acting capacity. This entails analyzing the characteristics and behavior of quartz without any external influences or modifications. The subsequent section outlines the outcomes derived from reinforcing quartz particles with fiber materials. This involves investigating the effects of integrating fiber materials into quartz, thereby enhancing its structural integrity and performance. By segregating the results into these two sections, a comprehensive evaluation of both quartz's standalone performance and its reinforced state is provided.

4.1.1 Fiber un-enforced Quartz bridging

The primary objective of this experiment was to assess the bridging capabilities of quartz particles when introduced into a drilling fluid. For this purpose, quartz particles within the size spectrum of 250 – 350 microns were carefully chosen. This range was slightly below the D50 value (315-355 microns) associated with the quartz particles.

To facilitate a comprehensive evaluation, the experiment incorporated three different slot sizes: 250, 300, and 400 microns. The selection of these slot sizes was intended to align the smallest and largest slot dimensions with the lower and upper boundaries, respectively, of the particle size spectrum ranging from 250-315 microns. This approach enabled the identification of the best- and worst-case scenarios, thus enabling a thorough analysis within the desired particle size range.

In each test, a total of three experiments were conducted. Each experiment involved the mixing of 4 grams of quartz particles with the specified size distribution, together with 200 grams of drilling fluid 1. It was crucial to initiate the test immediately after the particles were introduced into the drilling fluid. This precise timing was essential to ensure the particles remained uniformly dispersed within the fluid system, preventing them from settling at the bottom of the bridging apparatus (specifically, within the slot) before the commencement of the test.

It is important to highlight that currently, there is no standardized procedure or guideline provided by the American Petroleum Institute (API) for testing Lost Circulation Materials (LCM). Consequently, all bridging tests conducted in this study were limited to a duration of 20 minutes. This decision was based on previous experience, which demonstrated that LCM testing exceeding 25 minutes resulted in undesirable outcomes such as water breakthrough, loss of LCM, and drilling fluid due to bridge collapses (Belayneh & Aadnøy, 2022).

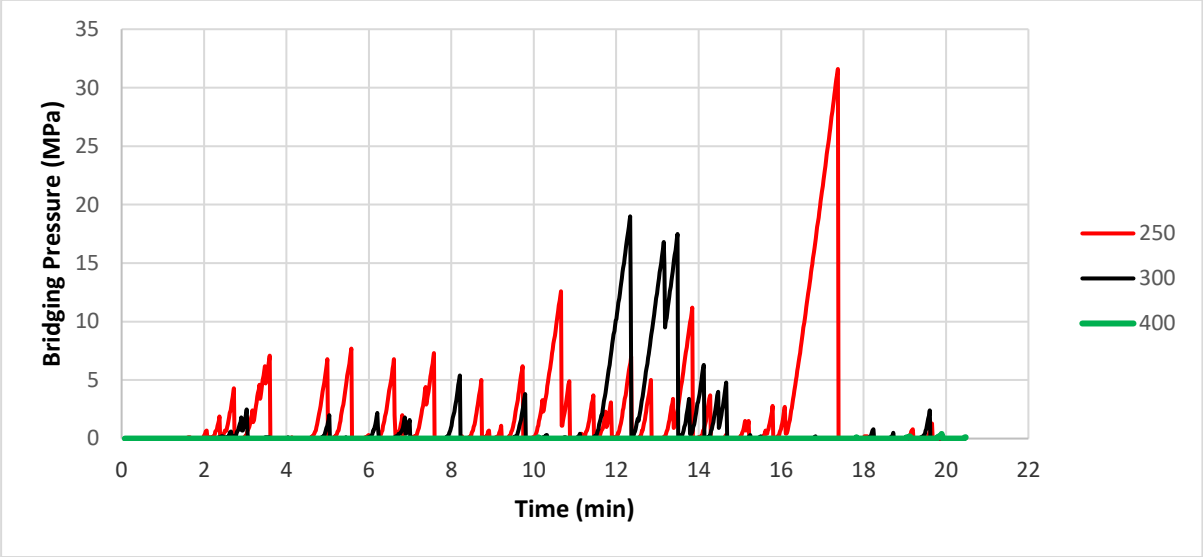

Figure 4.1: Quartz (250-315) Performance in Drilling Fluid 1

The analysis of the test results, as presented in the plot above, revealed several significant findings. Firstly, it was observed that the formation of the initial bridge at the slot opening typically occurred around 2 minutes after the commencement of the test, as depicted in the plot. This duration can be considered as the time required for the bridge to establish its initial structure. However, it should be noted that factors such as the density or concentration of the bridging particle (LCM) can influence this timing.

Each peak exhibited in the plot represents the maximum pressure that the respective bridge formed could withstand before collapsing. The chart clearly illustrates that the pressure resistance of bridges formed by quartz particles varied depending on the slot size. Particularly noteworthy is the fact that the bridge formed under the slot size of 250 microns exhibited the highest-pressure resistance compared to the bridges formed under the slot sizes of 300 and 400 microns. This observation suggests that the quartz particles effectively blocked the narrow 250-

micron slot and maintained their structural integrity even under high-pressure conditions of approximately 35 MPa.

In contrast, none of the bridges formed under the slot size of 400 microns could withstand a pressure close to 5 MPa. This outcome indicates that the bridging particles were unable to effectively block the wider slot and ultimately collapsed under the applied pressure, resulting in complete or total losses.

Furthermore, the plot clearly demonstrates a trend where the bridging performance of quartz particles decreased as the slot sizes increased. Consequently, weaker bridges were formed that could not withstand the applied pressure. This trend emphasizes the significant impact of slot size on the bridging performance of quartz particles in drilling fluid 1, thereby influencing the overall effectiveness of the bridging process.

4.1.2 Fiber Reinforcement of Quartz Bridging

It is worth noting that the complete losses encountered in the 400-micron slot were primarily attributed to the fact that the slot size exceeded the selected quartz particle size distribution. To enhance the performance, the particle was reinforced with wood fiber. The results of this reinforcement are displayed below.

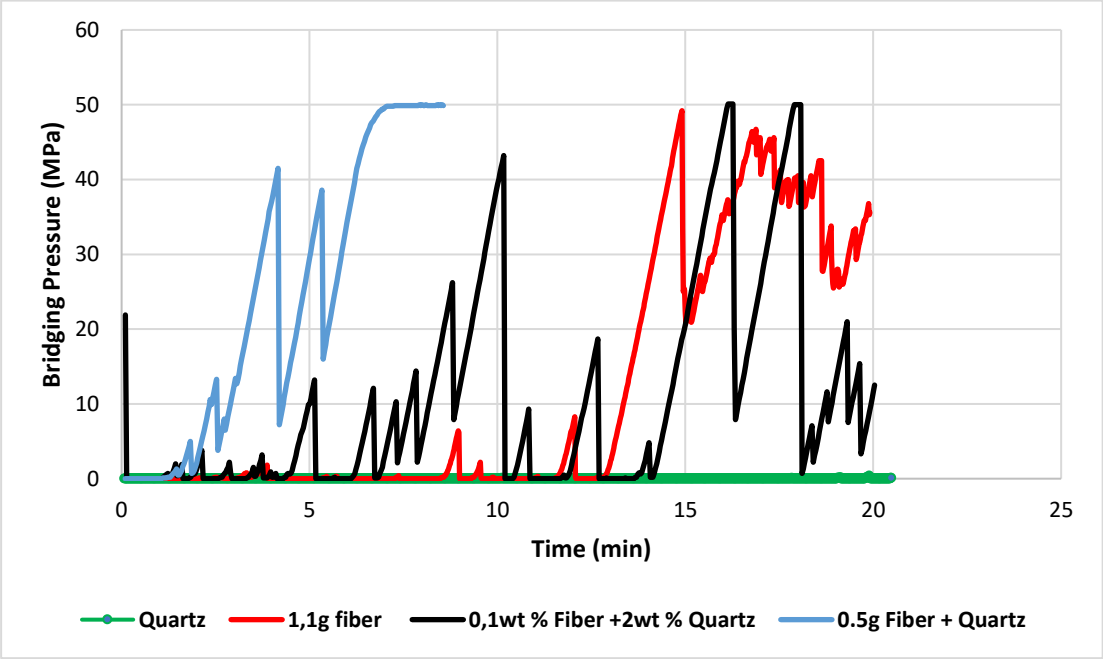

Figure 4.2: Effect of Fiber Reinforcement

The plot presented above provides a comprehensive comparison of the test results obtained from separate testing of fiber and quartz particles, as well as their composite results.

It is evident from the plot that the size of the quartz particles alone was insufficient to bridge the 400-micron slot, resulting in complete losses in this scenario. However, a separate test was conducted using a reduced concentration (1.1g) of wood fiber particles to evaluate their bridging effect. As observed in the plot, the fiber particles demonstrated significantly improved performance compared to the quartz particles. Although the slot was not completely plugged, the bridge formed by the fiber particles reached a peak pressure of 50 MPa, which was the maximum pressure specified for the experimental test, before collapsing.

An important observation pertains to the time required for the fiber particles to initiate bridging (pressure build-up). This can be attributed to the lightweight nature of the fiber material used, which resulted in a longer settling time for the fiber particles to effectively position themselves within the slot.

The slot was perfectly plugged when 4g of quartz particles were reinforced with 0.5g of fiber. However, this occurred within a shorter time interval compared to the time it took for the 1.5g of fiber particles to plug the slot. To optimize this outcome, a lower concentration of fiber was subsequently mixed with the same concentration of quartz. The result depicted in the plot above exhibited satisfactory performance and early plugging, although complete plugging was not achieved.

4.2 Effect of Quartz (whole particle size spectrum)

4.2.1 The Effect of Viscosity on Quartz Bridging Performance

For this experimental study we selected quartz particles with a size range of 0 to above 500 microns (entire particle size spectrum). The objective of this experimental investigation was to evaluate the impact of viscosity on the bridging performance of Quartz particle as Lost Circulation Material (LCM).

We utilized Drilling Fluid 2, which comprised three distinct types: Types A, B, and C, characterized by different rheological parameters. Type A fluid exhibited a lower viscosity compared to Type B and C fluids. Type B fluid, on the other hand, possessed a higher viscosity

than Type A, yet it was less viscous than Type C. Type C fluid stood out as the most viscous among the three.

For each fluid type, we conducted four individual tests, employing four carefully selected slot sizes: 150, 300, 450, and 650 microns. These slot sizes were chosen to encompass the entire range of particle sizes present in the quartz sample. In each test, we mixed 4 grams of whole-sized quartz particles with 200 grams of the corresponding fluid type. The duration of each test was constrained to 20 minutes, as mentioned previously.
We took precautions to prevent the premature settling of the bridging particles throughout the experiments.

The obtained results are presented in the subsequent plots, showcasing the relationship between viscosity and the bridging performance of the LCM.

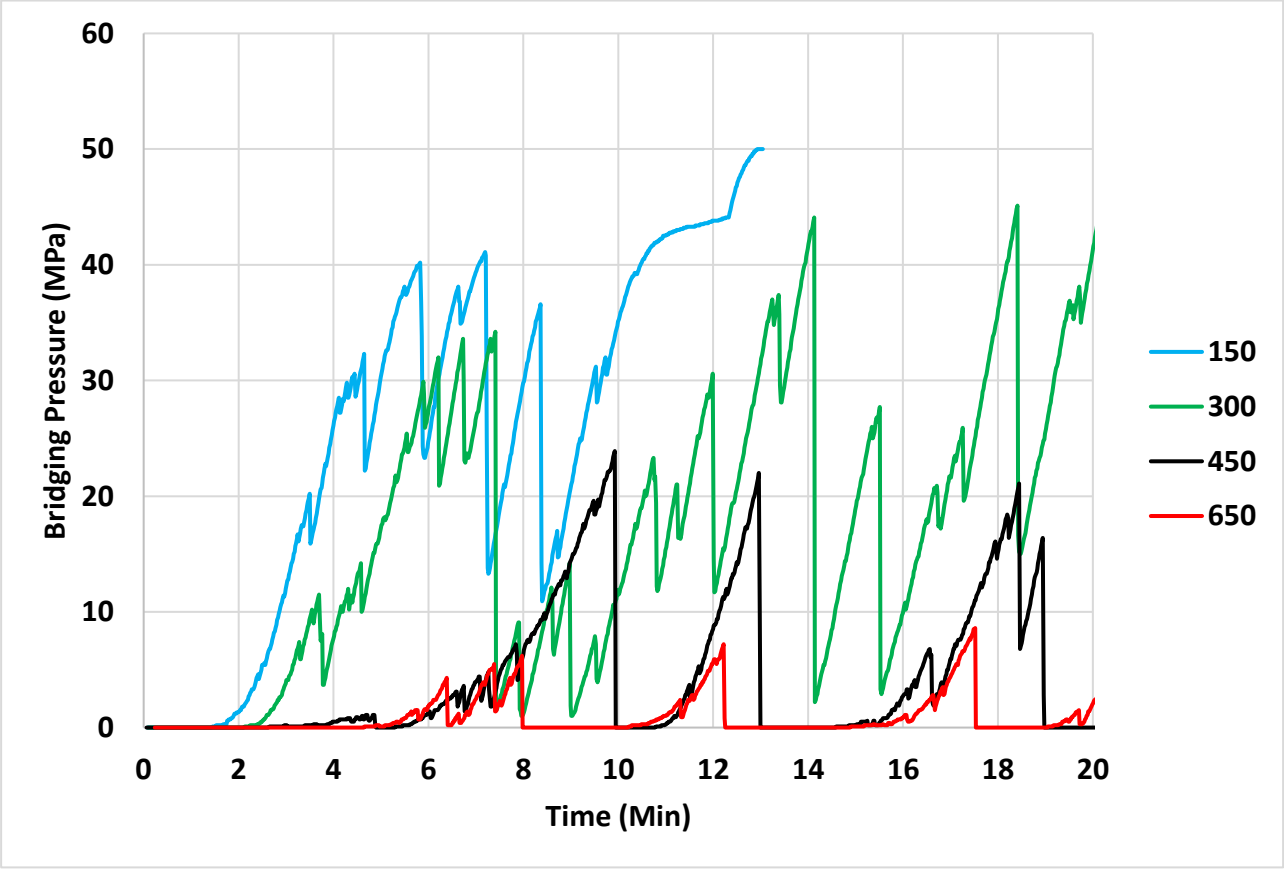

Figure 4.3: Quartz performance in (Type A fluid) 12.5 g Bentonite based fluid

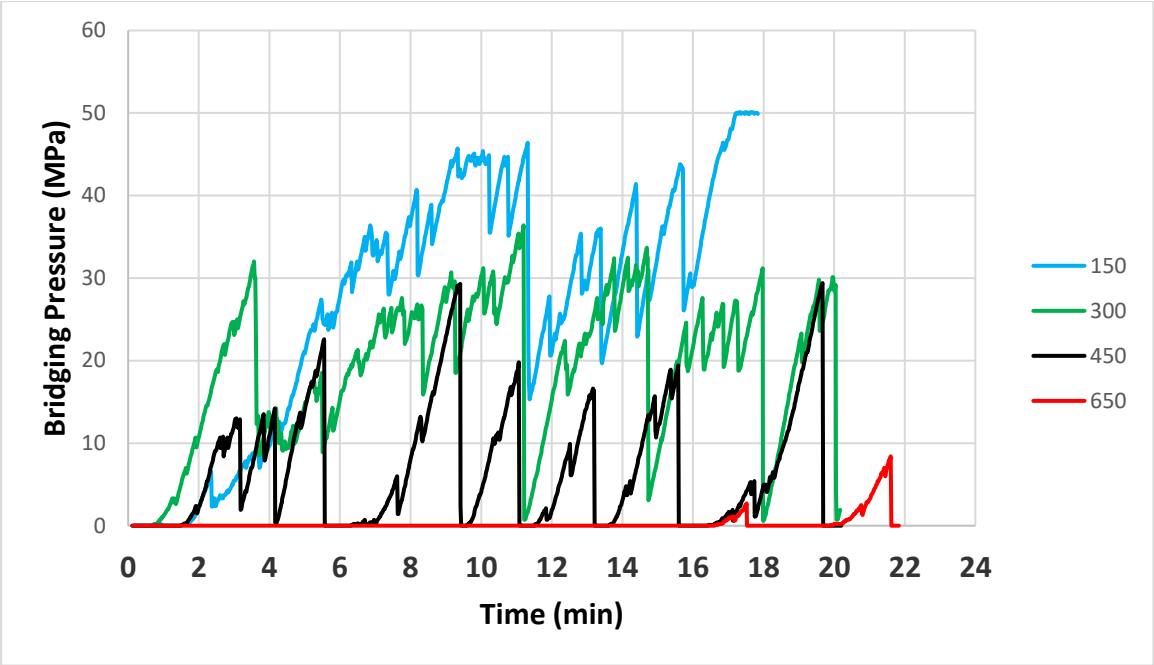

Figure 4.4: Quartz performance in (Type B fluid) 15 g Bentonite based fluid

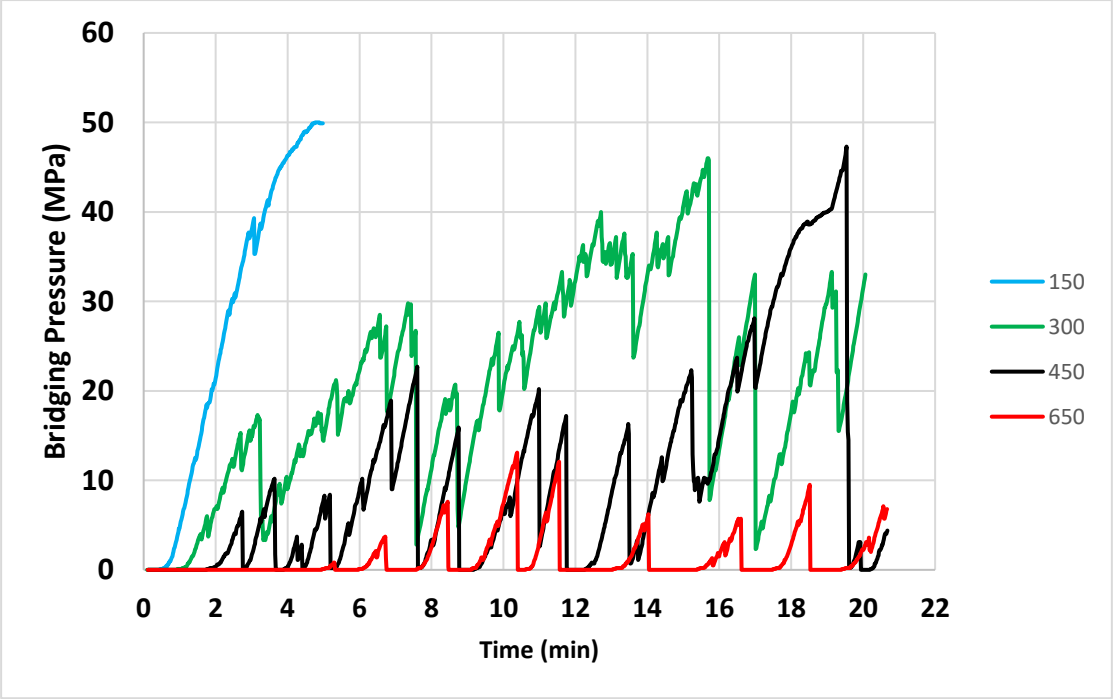

Figure 4.5: Quartz performance in (Type C fluid) 20 g Bentonite based fluid

Upon careful analysis of the provided plots, it is evident that quartz particles successfully sealed the openings in the 150-micron slot sizes for all three fluid systems, surpassing the predetermined maximum pressure threshold of 50 MPa established for the experimental study.

This outcome was anticipated due to the Particle Size Distribution (PSD) of quartz, which exhibited a D50 value within the 250–355-micron range, indicating that the majority of particles fell within this size range. It should be noted, however, that the time required for Types A and B fluids to achieve a perfect plug exhibited a series of peaks before finally achieving success after 13 minutes and 17 minutes, respectively. In contrast, Type C fluid, characterized by higher viscosity compared to Types A and B, achieved early plugging at approximately 5 minutes. This observation, along with other factors such as particle distribution within the fluid system, may influence the strength and nature of the formed bridge.

Furthermore, as the slot sizes increased, a consistent trend emerged across all three fluid types, indicating a diminishing performance of quartz particles. This finding suggests that larger slot sizes present a greater challenge for effective quartz bridging, corroborating the results obtained in previous experiments.

The bridging performance of quartz particles also displayed a noticeable correlation with the rheological parameters of the three fluid types, as illustrated in the performance plot. Specifically, it was observed that the bridging performance increased as the fluid viscosity increased from Type A to Type C fluids. However, a comprehensive analysis of these results, including an examination of the specific rheological parameters of each fluid type and their impact on the bridging behavior of quartz particles, will be presented in the forthcoming Data Analysis section. This analysis aims to provide a deeper understanding of the observed trends by exploring the interplay between particle properties, fluid characteristics, and rheology.

In conclusion, this experimental investigation focusing on the effect of viscosity on the bridging performance of quartz particles has provided valuable insights into the behavior of these particles under varying rheological conditions. The results demonstrate that quartz particles exhibit enhanced sealing capabilities in fracture openings within more viscous fluid systems compared to less viscous ones. The detailed analysis in the subsequent sections will further contribute to a comprehensive understanding of these phenomena.

4.2.2 Fiber Reinforcement

Building upon the previous experimental results focusing on reinforcing quartz with fiber, a comprehensive analysis was conducted to address the worst-case scenario involving a 650-micron slot size. This slot size demonstrated complete losses when utilizing quartz particles alone as the lost circulation material, highlighting the inefficiency of quartz particles in sealing

the 600-micron slot across the three aforementioned fluid types (A,B and C). In order to enhance the performance of quartz, an approach incorporating 1g of fiber reinforcement was implemented, and the ensuing results are presented in the following plot.

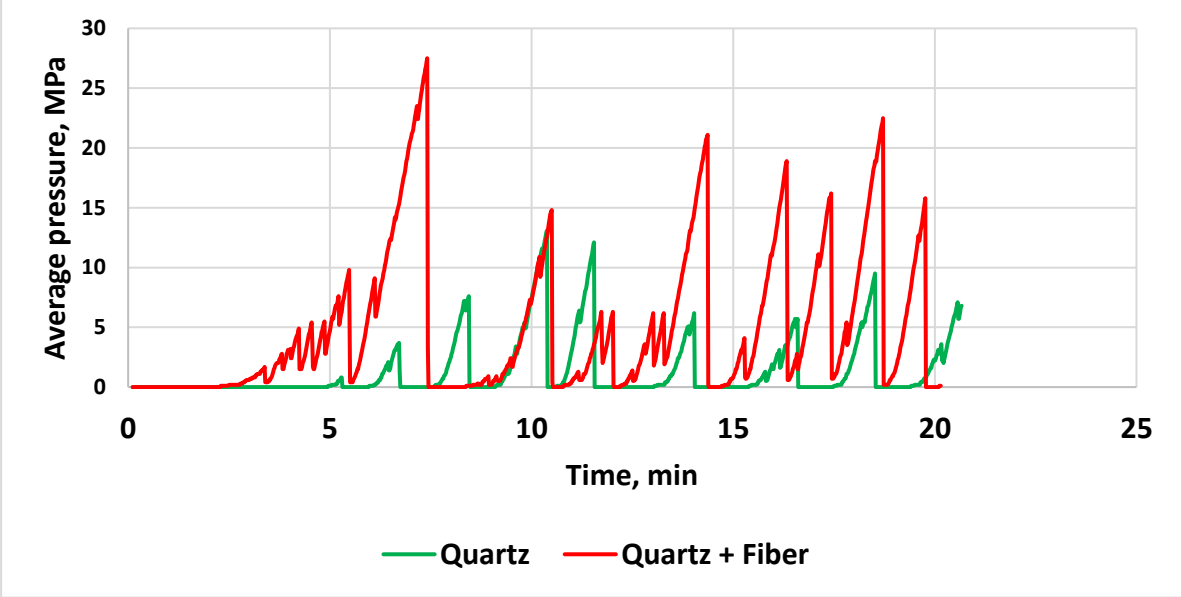

Figure 4.6: Quartz and Fiber performance on 650 µm slot Type C fluid

Firstly, it is worth noting that the quartz and fiber material exhibited early bridging attempts when compared to quartz particles alone. This agrees with earlier results from the 400micron slot and further reaffirms that the inclusion of fiber in the composition enhanced the bridging capabilities of the quartz particles.

Furthermore, the maximum pressure reached by the single acting quartz particles was approximately 15 MPa. However, when the quartz particles were reinforced with the addition of 1g of fiber, a remarkable increase in performance was observed, with the composite material achieving a maximum pressure of 30 MPa. This indicates a doubling of the maximum pressure achieved by the quartz particles alone, underscoring the effectiveness of the quartz and fiber composite.

Upon closer examination of the plot, it is evident that the composite material exhibited a more complex behavior compared to the single acting quartz particles. Multiple peaks were noticeable in the bridging performance of the composite material, suggesting a more dynamic and robust sealing mechanism. This contrasted with the relatively simpler behavior exhibited by the quartz particles alone.

In conclusion, the results obtained from the plot demonstrate that the composite material comprising quartz and fiber exhibited superior bridging performance when compared to the

single acting quartz particles. The early bridging attempts, higher maximum pressure achieved, and the presence of multiple peaks in the performance plot all indicate the enhanced effectiveness of the quartz and fiber composite. These findings highlight the advantages of reinforcing quartz particles with fiber to improve their bridging capabilities in practical applications.

4.2.3 The Effect of Lubricity on Quartz Bridging Performance

The objective of this experiment was to assess the influence of lubricity on the bridging performance of Quartz particles. As previously mentioned, the drilling fluid system used in this test was formulated by incorporating two types of lubricants into a reference fluid, as explained in the drilling fluid synthesis section regarding lubricity testing. The purpose of adding these lubricants was to introduce variations in the Coefficient of Friction (COF) of the fluid system, enabling the investigation of the lubricant's impact in each case.

For this test, 4g of whole-sized Quartz particles within the Particle Size Distribution (PSD) range of 0-500 microns were mixed with 200g of two fluid types: Base Oil Lube and Base Oil + Graphite Lube, having COF values of 0.38 and 0.28, respectively. The test was conducted using a slot size of 300 microns, which was determined from previous experiments to demonstrate favorable bridging performance with the selected Quartz particles. Consistent with the customary duration, the test was limited to 20 minutes, and the results are presented in the following plot.

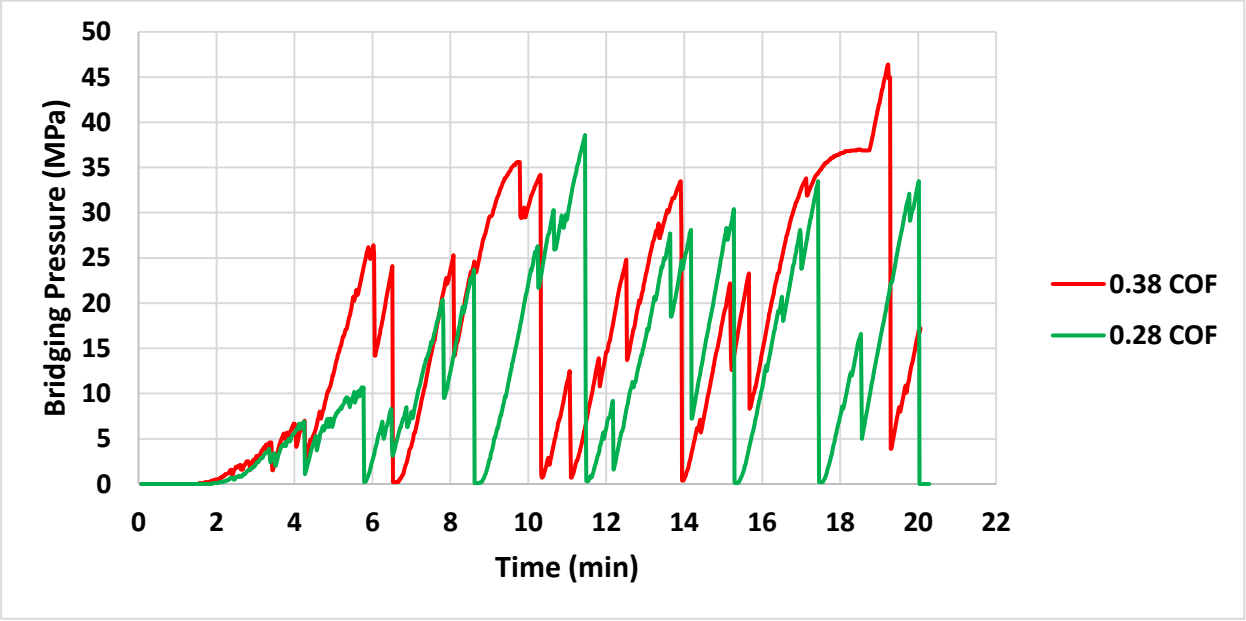

Figure 4.7: Effect of Lubricity on Quartz Performance on 300 slot size

From the plot, it can be observed that the Base Oil Lube, with a COF of 0.38, exhibited the highest peak pressure of approximately 48 MPa, whereas the Graphite-treated Base Oil Lube, with a lower COF of 0.28, demonstrated a lower maximum peak pressure close to 40 MPa. However, both fluid systems exhibited multiple peaks. It is noteworthy that the fluid with the lower COF resulted in the formation of several peaks, indicating that the bridges formed by the Quartz particles in the Graphite-treated Base Oil Lube were unstable and prone to collapse. A comprehensive analysis of these obtained data is presented in the Data Analysis section of this study.

5 Data Analysis of Test Results

This study adopts a comprehensive data analysis methodology developed by Toroqi for particle plugging tests. This methodology was designed to extract richer knowledge on the performance of drilling fluids and to gain a deeper insight into the capabilities of particles in plugging fractures. The aim is to develop a set of parameters that can be used to evaluate the sealing potential of drilling fluids.

Out of the eight parameters defined by Toroqi, this study focuses on four parameters that provide quantitative information on the performance of particles in terms of particle plugging and resistance. These parameters are maximum pressure, average pressure, total number of peaks, and average peak pressure.

1. **Maximum pressure** is a crucial parameter that reflects the maximum pressure recorded during the test. This parameter can be influenced by factors such as the distribution of particles in the fluid system and on the surface of the slot opening, strength of the particle or LCM, lubricity, viscosity and other factors yet to be investigated.
2. **Average pressure**, on the other hand, provides a qualitative measure of the overall performance of the particles in the drilling fluids. It reveals information about the average strength of the bridge formed during the test and can be used to compare the strengthening capabilities of different drilling fluids. It comprises of the peak build up and collapse pressure.
3. **Total number of peaks** represents the ability of the fluid to form a plug, irrespective of its strength. Each peak in the pressure plot shows the collapse of a bridge formed during the test.
4. **Average peak pressure**, on the other hand, is the average strength of the plugs formed by the fluid. This parameter is critical in analyzing particle plugging test results and provides information on the strengthening capability of the LCM system.

The data analysis methodology and parameters defined in this study will be adopted in future studies to evaluate the sealing potential of drilling fluids and to extract richer knowledge on the performance of the fluid. The parameters can also be used to compare the performance of different drilling fluids in terms of particle plugging and resistance. Finally, optimizing drilling fluid formulations for better performance in the field is achievable with the use of these

parameters [64]. Thus, this study provides a solid foundation for the evaluation and optimization of drilling fluids for efficient particle plugging and resistance.

As outlined earlier in the experimental study plan, we applied the methodology described by Toroqi to analyze the result obtained in the above test. Detailed analysis and comparison will be made in this section, to explain correlations and trends observed.

Average Pressure was selected as the primary parameter of comparison since it provides a qualitative measure of the overall performance of the particles in the drilling fluids.

5.1 Data Analysis of Quartz Particle Bridging Performance (250 – 315 microns)

From the obtained results, the maximum pressure, average pressure, average peak pressure, and total number of peaks across the 250-, 300-, and 400-micron slots were calculated using a calculator generated in Excel, and the results are presented in the Table 5.1.

Table 5.1: Pressure values for quartz (250 – 315 micron) test across varying slot sizes.

Slot size	Maximum Pressure	Average Pressure	Average Peak Pressure	Total Number of Peaks
250	31.6	2.0	3.8	38
300	19.0	1.1	4.20	23
400	0.4	0.0	0	0

The average pressure was selected and presented as the parameter of comparison since it represents the average performance of all the materials present in the fluid system, while the other 3 parameters, (max pressure, average peak pressure, and the number of peaks) can be affected by several factors which can include, the position of the bridging material on the slot, the nature of the bridging material related to the size of the material (fiber) present in or on the slot, the weight, and other possible factors.
The plots of the Average pressure of the varying slot sizes are presented below, for comparison of the other parameters refer to the index or appendix section.

Figure 5.1: Average Bridging pressure across 3 slot sizes

The analysis of the plot data reveals significant observations regarding the relationship between slot size and the measured parameter (Pave):

1. ***Decreasing Pave with Increasing Slot Size:*** A clear decreasing trend in Pave values is observed as the slot size increases from 250 to 400. This indicates a negative correlation between slot size and system performance, suggesting that larger slot sizes result in lower average bridging pressure.
2. ***Negative Impact of Larger Slot Sizes***: The inverse relationship between slot size and Pave values highlights the detrimental effect of larger slot sizes on system performance. Factors such as reduced particle bridging, decreased sealing efficiency, or compromised structural integrity could contribute to this negative impact.

These observations can be attributed to the difference between the slot size and the size of the bridging particles. A larger difference makes it more challenging for particles to accumulate and form a stable bridge, leading to increased losses. Additionally, factors such as fluid properties and structural considerations should be considered in understanding the observed behavior.

In conclusion, the plot analysis demonstrates that larger slot sizes negatively impact fluid system performance, resulting in decreased average bridging pressure values. These findings highlight the importance of optimizing the particle performance by considering factors such as particle size distribution, fluid properties, and addition of a reinforcing material (fiber) to enhance system performance and minimize losses.

5.2 Analysis of the fibre reinforcement effect

As shown in Figure 5.1, the 2 wt % Quartz (250-315 μm) at the 400-micron slot exhibited a total fluid loss. This can be attributed to the fact that the D50 value of the quartz particles is smaller than the width of the slot. To enhance the performance characteristics of Quartz, a comprehensive evaluation was conducted to assess the individual impact of Quartz and its combined effects with fiber. The plot below shows a comparison of experimental results obtained from technical analysis conducted to understand the relationship between different weight percentages of quartz and fiber and their corresponding average sustained pressure values (measured in Mega Pascals, MPa)

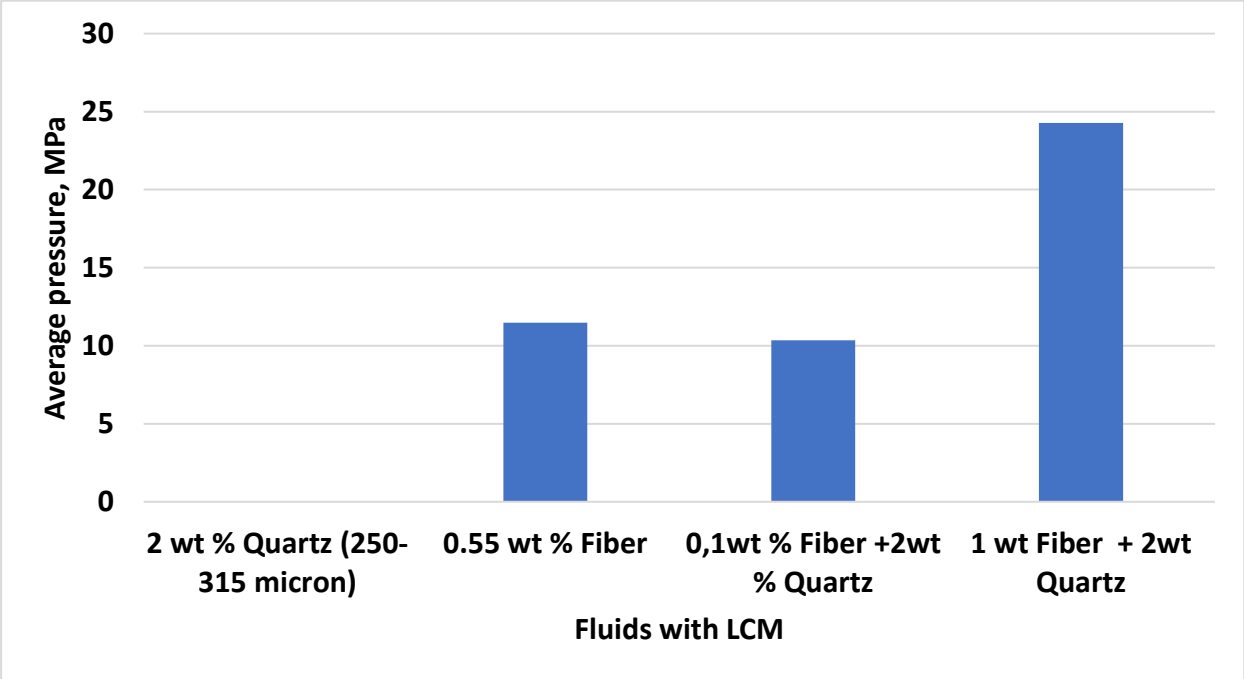

Figure 5.2: Average Pressure on 400microns slot

Upon analyzing the data presented in the plot, several important observations can be made:

1. Effect of Quartz Alone: The composition containing 2 wt % quartz alone (250-315 microns) had a zero average pressure. This suggests that when quartz particles are used as the sole component, they do not contribute significantly to sustaining average pressure. The absence of fiber in this composition may limit its bridging capability and overall stability.
2. Impact of Fiber in Combination with Quartz: When 0.1 wt % fiber is added along with 2 wt % quartz, the average bridging pressure increases to 10 MPa. This indicates that the inclusion of a small percentage of fiber enhances the performance compared to using

quartz alone. The fibers likely play a crucial role in improving the bridging capability and overall stability of the composition, resulting in enhanced performance.

3. Enhanced Performance with Higher Fiber and Quartz Content: The composition with 1 wt % fiber and 2 wt % quartz demonstrates the highest performance value of 24. This indicates that increasing the concentrations of both fiber and quartz further enhances performance. The higher content of both components likely contributes synergistically to improve the stability, bridging ability, or other relevant factors, resulting in significantly higher performance.
4. Performance with 0.55 wt % Fiber: The composition with 0.55 wt % fiber alone yields a performance value of 11. This indicates that using a relatively higher percentage of fiber without the presence of quartz also contributes to improved performance compared to quartz alone. The fibers in this composition likely play a significant role in enhancing the performance parameter.

In conclusion, the analysis of the table data reveals that the inclusion of fiber, either in combination with quartz or on its own, significantly enhances the performance compared to using quartz alone. The combined presence of fiber and quartz at higher concentrations leads to the highest performance value, suggesting a synergistic effect. Additionally, the individual presence of a higher percentage of fiber without quartz also yields improved performance. These findings highlight the importance of considering the composition and concentration of quartz and fiber to optimize performance in relevant applications, ensuring better stability, bridging ability, and overall performance of the material system.

5.3 Data Analysis of Viscosity Effect on Bridging Performance of Quartz.

The purpose of this analysis is to examine the relationship between the average pressure sustained across different slot sizes and the rheological parameters of three fluid types: Type A, Type B, and Type C. The rheological parameters considered include yield strength, plastic viscosity, low shear yield strength, and the K parameter. By evaluating the calculated values of these parameters, we aim to identify trends and correlations with the average pressure data.

Table 5.2: calculated rheological parameters for Type A, B, and C fluids.

Fluid type	Yield Strength	Plastic Viscosity	Low Shear Yield Strength	Consistency index
Type A	9	4	5.5	1.165
Type B	12.5	6	8.5	1.475
Type C	18	6.6	12.5	2.952

The table provided above lists the rheological parameters for each fluid type.

Table 5.3: Average Pressure values for varying fluid types on different slot sizes.

Slot	Type A	Type	Type C
150	25,42	26,67	27,58
300	17	18,95	20,34
450	4,17	6,8	10,5
650	0,88	0,05	1,3

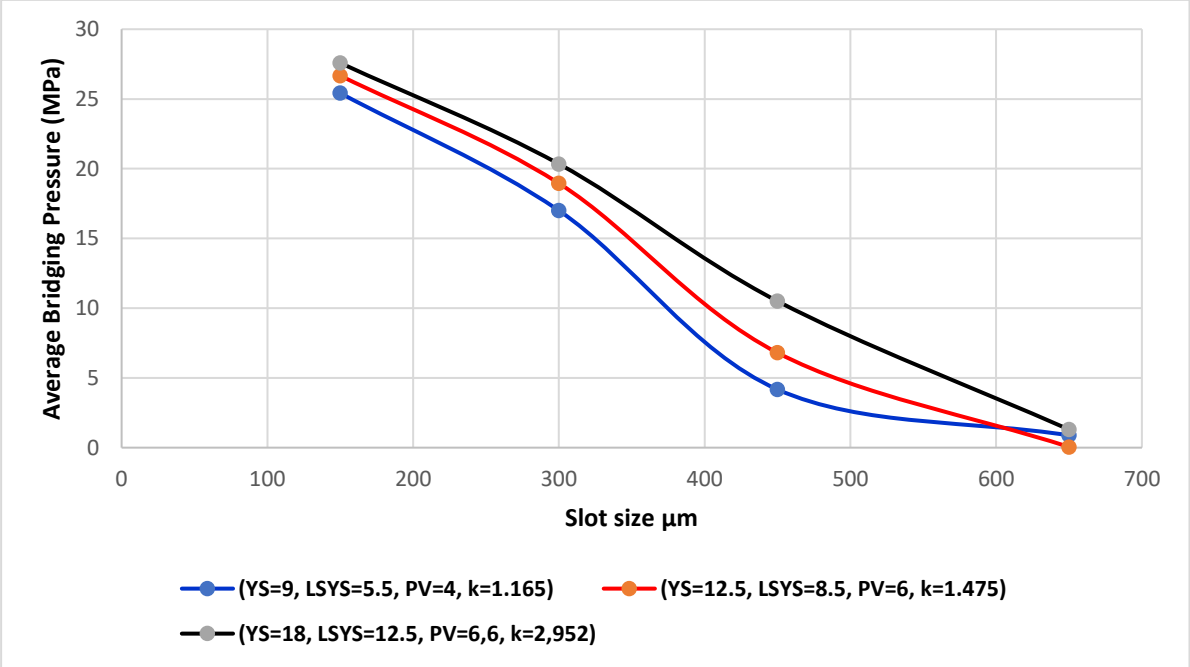

Figure 5.3: Average Bridging Pressure in varying fluids rheology for various slot sizes

On analyzing the plot for the average bridging pressure sustained across varying slot sizes for each fluid rheological parameter, the following observations were made.

Yield Strength (YS):

An increase in yield strength corresponds to an increase in the average bridging pressure. As can be seen in the 150-micron slot, as the yield point increased from 9 to 12.5 and 18, the

average pressure showed an increasing response of 25.42, 26.67, and 27.5 respectively. This indicates that as the fluids' yield strength increases, they require higher pressures to initiate flow. This trend is consistent across all slot sizes and fluid types.

Plastic Viscosity (PV):

Similarly, an increasing trend between plastic viscosity and the average bridging pressure is observed. As the fluid's resistance to flow, represented by plastic viscosity, increases, the average pressure needed to initiate fluid loss through the bridge also increases. This relationship is evident for all slot sizes and fluid types.

Low Shear Yield Strength (LSYS):

The low shear yield strength also demonstrates a positive correlation with the average pressure. Fluids with higher low shear yield strength values such as Type C fluid, require higher pressures to initiate flow. This trend is consistent across all fluid types and slot sizes.

Consistency index (K):

The average pressure increases with higher values of the consistency index, indicating a greater ability to resist flow compared to resistance to shearing forces. This suggests that as the consistency index increases across the 3 fluids, the fluid system exhibits increased resistance to fluid loss, resulting in higher average pressure requirements.

Based on the analysis of the observed trends, it can be concluded that there is a correlation between the rheological properties (yield strength, plastic viscosity, low shear yield strength, and consistency index) and the average pressure sustained across different slot sizes. The higher the rheological parameters, the higher the average pressure sustained by the fluid system. These findings highlight the importance of considering rheological properties when designing drilling fluids to ensure optimal performance in various drilling operations.

5.4 Data Analysis of Lubricity Effect on Bridging Performance of Quartz.

In this section, the analysis focuses on investigating the impact of fluid lubricity on the average bridging pressure. Lubricity, in this study, is quantified by considering the coefficient of friction (COF), which serves as a measure of the resistance encountered during sliding or relative motion between two surfaces. By evaluating the COF, we can gauge the lubricating properties

of a substance or material, with lower COF values indicating enhanced lubricity characterized by reduced friction and smoother movement between the surfaces.

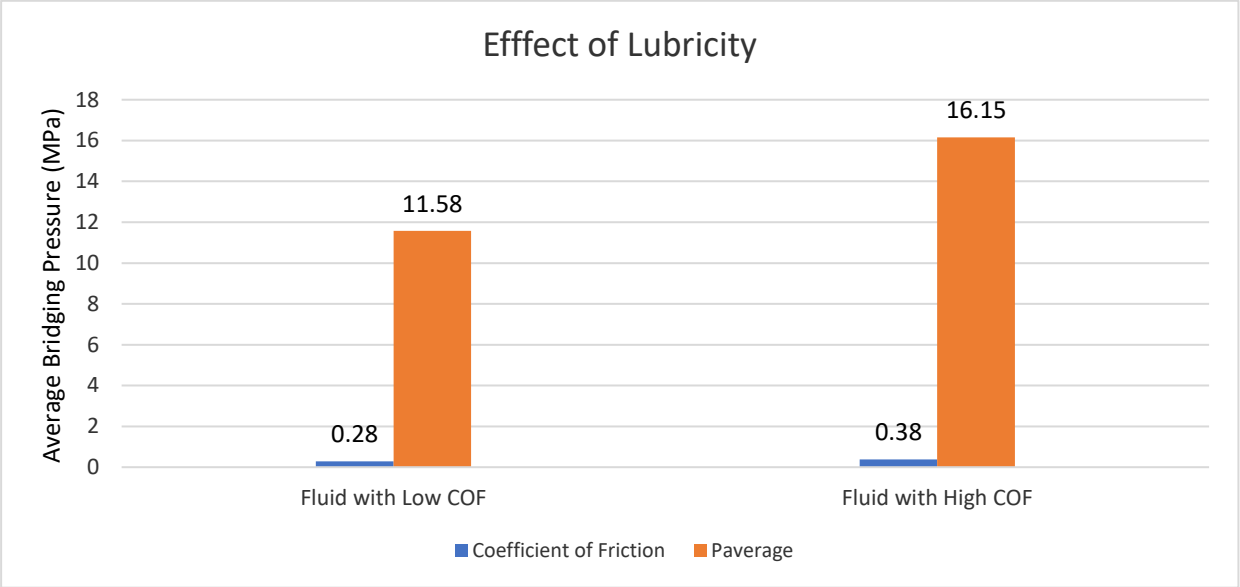

Figure 5.4: Effect of Lubricity

Examining the obtained results, two fluid types are compared based on their COF values. The fluid with a lower COF of 0.28 exhibits an average bridging pressure of approximately 11.6 MPa, whereas the fluid with a higher COF of 0.38 demonstrates a notably higher average bridging pressure of 16.2 MPa. These findings suggest a correlation between the bridging performance of the particles in the fluid and the lubricity of the fluid system.

The observed relationship implies that the fluid with low lubricity, as indicated by high COF, possesses improved bridging capabilities, resulting in higher average bridging pressure values. Conversely, the fluid with higher lubricity, represented by low COF, exhibits a reduced bridging performance, leading to a comparatively lower average bridging pressure.

These findings emphasize the significance of fluid lubricity in relation to bridging performance, highlighting the role of reduced friction and smoother motion in facilitating effective particle bridging within the fluid system. Understanding and optimizing lubricity can contribute to the design and selection of fluids with enhanced bridging properties, ultimately enhancing their performance in various applications where particle bridging is critical.

6 Summary and Conclusion

This study investigated the effect of quartz particles on bridging performance, with a subsequent focus on exploring the influence of viscosity and lubricity on bridging behavior. Fiber reinforcement was also examined to enhance the performance of quartz particles.

- The results revealed that fiber reinforcement significantly improved the bridging performance of quartz particles.
- When studying the effect of viscosity, a consistent trend was observed across multiple parameters. Increasing parameters such as yield strength, plastic viscosity, low shear yield strength, and the consistency index led to an increase in average bridging pressure across various slot sizes.
- Moreover, the investigation into lubricity revealed an interesting finding. The fluid with a higher coefficient of friction (indicating reduced lubricity) exhibited superior bridging performance compared to the fluid with a lower coefficient of friction.

In conclusion, this research underscores the importance of fiber reinforcement in enhancing the bridging performance of quartz particles. It also highlights the significant influence of viscosity and lubricity on the behavior of such systems. These findings provide valuable insights for optimizing and improving the performance of quartz-based LCM systems in practical applications.

Overall, this study contributes to advancing the understanding of bridging performance in quartz particle systems, shedding light on key factors that can be manipulated/optimized to achieve desired outcomes.

7 References

[1] M. S. Aston, M. W. Alberty, M. R. McLean, H. J. De Jong, and K. Armagost, "Drilling Fluids for Wellbore Strengthening," *Proceedings of the Drilling Conference*, pp. 321–328, Mar. 2004, doi: 10.2118/87130-MS.

[2] A. T. T. Al-Hameedi, H. H. Alkinani, S. Dunn-Norman, R. E. Flori, and S. A. Hilgedick, "Real-time lost circulation estimation and mitigation," *Egyptian Journal of Petroleum*, vol. 27, no. 4, pp. 1227–1234, Dec. 2018, doi: 10.1016/J.EJPE.2018.05.006.

[3] "Gabi paper AADE-03-NTCE-38-Ivan".

[4] H. H. Alkinani, A. Taleb, T. Al-Hameedi, and S. Dunn-Norman, "IPTC-19877-MS State-of-the-Art Review of Lost Circulation Materials and Treatments-Part II: Probability and Cost Analyses," 2020. [Online]. Available: http://onepetro.org/IPTCONF/proceedings-pdf/20IPTC/3-20IPTC/D031S064R001/1188371/iptc-19877-ms.pdf/1

[5] J. M. Davison *et al.*, "Extending the Drilling Operating Window in Brent: Solutions for Infill Drilling in Depleting Reservoirs," *Proceedings of the Drilling Conference*, pp. 647–656, Mar. 2004, doi: 10.2118/87174-MS.

[6] N. Pilisi, Y. Wei, and S. A. Holditch, "Selecting Drilling Technologies and Methods for Tight Gas Sand Reservoirs," *SPE/IADC Drilling Conference, Proceedings*, vol. 1, pp. 276–295, Feb. 2010, doi: 10.2118/128191-MS.

[7] F. B. Growcock, "Stabilizing the wellbore to prevent lost circulation," *researchgate.net*, 2011, Accessed: Jun. 01, 2023. [Online]. Available: https://www.researchgate.net/profile/Frederick-Growcock/publication/290592459_Stabilizing_the_wellbore_to_prevent_lost_circulation/links/590e1b0f458515978185c5f3/Stabilizing-the-wellbore-to-prevent-lost-circulation.pdf

[8] S. M. Gandhi and B. C. Sarkar, "Drilling," *Essentials of Mineral Exploration and Evaluation*, pp. 199–234, Jan. 2016, doi: 10.1016/B978-0-12-805329-4.00015-6.

[9] "Drilling fluid - AAPG Wiki." https://wiki.aapg.org/Drilling_fluid (accessed May 24, 2023).

[10] M. Khodja, M. Khodja-Saber, J. Paul, N. Cohaut, and F. Bergay, "Drilling Fluid Technology: Performances and Environmental Considerations," *Products and Services; from R&D to Final Solutions*, Nov. 2010, doi: 10.5772/10393.

[11] "Water-Based Mud Ultimate Guide - Drilling Manual." https://www.drillingmanual.com/water-based-drilling-mud-types-application/?utm_content=cmp-true (accessed May 24, 2023).

[12] "saltwater mud | Energy Glossary." https://glossary.slb.com/en/terms/s/saltwater_mud (accessed May 24, 2023).

[13] A. Patel, E. Stamatakis, S. Young, and J. Friedheim, "Advances in inhibitive water-based drilling fluids - Can they replace oil-based muds?," *Proceedings - SPE International Symposium on Oilfield Chemistry*, pp. 614–621, 2007, doi: 10.2118/106476-MS.

[14] "What is Oil-Based Drilling Mud (OBM)? - Definition from Trenchlesspedia." https://www.trenchlesspedia.com/definition/4528/oil-based-drilling-mud-obm (accessed May 24, 2023).

[15] "Engineer's Guide to Oil Field Chemicals and Fluids."

[16] O. E. Agwu *et al.*, "A critical review of drilling mud rheological models," *J Pet Sci Eng*, vol. 203, p. 108659, 2021, doi: 10.1016/j.petrol.2021.108659.

[17] A. C. Obinna, G. O. Mbah, and M. I. Onoh, "Optimization and Process Modeling of Viscosity of Oil Based Drilling Muds," *Journal of Human, Earth, and Future*, vol. 2, no. 4, pp. 412–423, Dec. 2021, doi: 10.28991/HEF-2021-02-04-09.

[18] Bourgoyne, A.J.T., Chenevert , M.E. & Millheim, K.K., 1986. SPE Textbook Series, Volume 2: Applied Drilling Engineering, Society of Petroleum Engineers.

[19] R. E. Robertson and H. A. Stiff, "An Improved Mathematical Model for Relating Shear Stress to Shear Rate in Drilling Fluids and Cement Slurries," *Society of Petroleum Engineers Journal*, vol. 16, no. 01, pp. 31–36, Feb. 1976, doi: 10.2118/5333-PA.

[20] "What is Shear Rate and Why is it Important? | Labcompare.com." https://www.labcompare.com/10-Featured-Articles/338534-What-is-Shear-Rate-and-Why-is-it-Important/ (accessed May 25, 2023).

[21] G. V. Chilingarian *et al.*, "Drilling Fluid Evaluation Using Yield Point-Plastic Viscosity Correlation," *http://dx.doi.org/10.1080/00908318608946052*, vol. 8, no. 2–3, pp. 233–244, Jan. 2007, doi: 10.1080/00908318608946052.

[22] F. Alakbari, S. Elkatatny, M. S. Kamal, and M. Mahmoud, "Optimizing the Gel Strength of Water-Based Drilling Fluid Using Clays for Drilling Horizontal and Multi-Lateral Wells," *Society of Petroleum Engineers - SPE Kingdom of Saudi Arabia Annual Technical Symposium and Exhibition 2018, SATS 2018*, Apr. 2018, doi: 10.2118/192191-MS.

[23] "Viscosity of Newtonian and Non-Newtonian Fluids." https://www.rheosense.com/applications/viscosity/newtonian-non-newtonian (accessed Jun. 01, 2023).

[24] J. R. A. Pearson, "Dynamics of Polymeric Liquids. Volume 1. Fluid Mechanics. By R. B. BIRD, R. C. ARMSTRONG and 0. HASSAGER. 470 pp. 222.00. Volume 2. Kinetic Theory. By R. B. BIRD, 0. HASSAGER, R. C. ARMSTRONG and C. F. CURTISS. 257 pp. £20.00. Wiley, 1977.," *J Fluid Mech*, vol. 86, no. 1, pp. 204–207, May 1978, doi: 10.1017/S0022112078211081.

[25] "(PDF) Testing and modeling of the thixotropic behavior of cementitious materials." https://www.researchgate.net/publication/323616085_Testing_and_modeling_of_the_thixotropic_behavior_of_cementitious_materials (accessed Jun. 03, 2023).

[26] R. P. Chhabra, "Non-Newtonian fluids: An introduction," *Rheology of Complex Fluids*, pp. 3–34, 2010, doi: 10.1007/978-1-4419-6494-6_1/COVER.

[27] "Drilling Fluids Rheological Models | Drilling Course." https://www.drillingcourse.com/2020/04/drilling-fluids-rheological-models.html (accessed Jun. 01, 2023).

[28] "Bingham plastic model | Download Scientific Diagram." https://www.researchgate.net/figure/Bingham-plastic-model_fig3_323616085 (accessed Jun. 07, 2023).

[29] R. Caenn, H. C. H. Darley†, and G. R. Gray†, "The Rheology of Drilling Fluids," *Composition and Properties of Drilling and Completion Fluids*, pp. 151–244, 2017, doi: 10.1016/B978-0-12-804751-4.00006-7.

[30] Ochoa M.V. (2006)Analysis of Drilling Fluid Rheology and Tool Joint Effect to Reduce Errors in Hydraulics Calculations. PhD Dissertation, Texas A&M University, College Station, Texas (August 2006).

[31] F. B. Growcock, "Stabilizing the wellbore to prevent lost circulation Wellbore Stability : Fluid-Shale Compatibility View project Modeling and Control of Managed Pressure Drilling View project," 2011. [Online]. Available: https://www.researchgate.net/publication/290592459

[32] M. Lesage, P. Hall, J. R. A. Pearson, and M. J. Thiercelin, "Pore-Pressure and Fracture-Gradient Predictions," *Journal of Petroleum Technology*, vol. 43, no. 06, pp. 652–654, Jun. 1991, doi: 10.2118/21607-PA.
[33] A. M. Raaen, P. Horsrud, H. Kjørholt, and D. Økland, "Improved routine estimation of the minimum horizontal stress component from extended leak-off tests," *International Journal of Rock Mechanics and Mining Sciences*, vol. 43, no. 1, pp. 37–48, Jan. 2006, doi: 10.1016/J.IJRMMS.2005.04.005.
[34] B. Sigve. Aadnøy, *Modern well design*. CRC Press/Balkema, 2010.
[35] Y. Feng, J. F. Jones, and K. E. Gray, "A Review on Fracture-Initiation and -Propagation Pressures for Lost Circulation and Wellbore Strengthening," *SPE Drilling & Completion*, vol. 31, no. 02, pp. 134–144, May 2016, doi: 10.2118/181747-PA.
[36] T. R. Bratton, I. M. Rezmer-Cooper, J. Desroches, Y. E. Gille, Q. Li, and M. McFayden, "How to Diagnose Drilling Induced Fractures in Wells Drilled with Oil-Based Muds with Real-Time Resistivity and Pressure Measurements," *Proceedings of the Drilling Conference*, vol. 1, pp. 382–391, Feb. 2001, doi: 10.2118/67742-MS.
[37] R. Aguilera, "Geologic aspects of naturally fractured reservoirs," *Leading Edge (Tulsa, OK)*, vol. 17, no. 12, p. 1667, 1998, doi: 10.1190/1.1437912.
[38] W. Deng *et al.*, "Permeability prediction for unconsolidated hydrate reservoirs with pore compressibility and porosity inversion in the northern South China Sea," *J Nat Gas Sci Eng*, vol. 95, p. 104161, Nov. 2021, doi: 10.1016/J.JNGSE.2021.104161.
[39] E. van Oort, J. Gradishar, G. Ugueto, K. M. Cowan, K. K. Barton, and J. W. Dudley, "Accessing Deep Reservoirs by Drilling Severely Depleted Formations," Feb. 2003, doi: 10.2118/79861-MS.
[40] B. E. Carson, "Lost Circulation Treatments for Naturally Fractured, Vugular, or Cavernous Formations," *Society of Petroleum Engineers of AIME, (Paper) SPE*, pp. 155–166, Mar. 1985, doi: 10.2118/13440-MS.
[41] "Various Lost Circulation Zone Types [2] | Download Scientific Diagram." https://www.researchgate.net/figure/Various-Lost-Circulation-Zone-Types-2_fig1_366718374 (accessed Jun. 03, 2023).
[42] M. Belayneh and B. Aadnøy, "Bridging performances of lost circulation materials (LC-LUBE and mica) and their blending in 80/20 and 60/40 oil-based drilling fluids," *Front Phys*, vol. 10, Nov. 2022, doi: 10.3389/fphy.2022.1042242.
[43] M. I. Magzoub, S. Salehi, I. A. Hussein, and M. S. Nasser, "Loss circulation in drilling and well construction: The significance of applications of crosslinked polymers in wellbore strengthening: A review," *J Pet Sci Eng*, vol. 185, p. 106653, Feb. 2020, doi: 10.1016/J.PETROL.2019.106653.
[44] L. Pu, P. Xu, M. Xu, J. Song, and M. He, "Lost circulation materials for deep and ultra-deep wells: A review," *J Pet Sci Eng*, vol. 214, p. 110404, Jul. 2022, doi: 10.1016/J.PETROL.2022.110404.
[45] K. R. Klungtvedt and A. Saasen, "The Role of Particle Size Distribution for Fluid Loss Materials on Formation of Filter-Cakes and Avoiding Formation Damage," *Journal of Energy Resources Technology, Transactions of the ASME*, vol. 145, no. 4, Apr. 2023, doi: 10.1115/1.4056187.
[46] A. Abrams, "Mud Design To Minimize Rock Impairment Due To Particle Invasion," *Journal of Petroleum Technology*, vol. 29, no. 05, pp. 586–592, May 1977, doi: 10.2118/5713-PA.
[47] M. A. Dick, T. J. Heinz, C. F. Svoboda, and M. Aston, "Optimizing the Selection of Bridging Particles for Reservoir Drilling Fluids," Feb. 2000, doi: 10.2118/58793-MS.
[48] S. Vickers, M. Cowie, T. Jones, and A. J. Twynam, "A NEW METHODOLOGY THAT SURPASSES CURRENT BRIDGING THEORIES TO EFFICIENTLY SEAL

A VARIED PORE THROAT DISTRIBUTION AS FOUND IN NATURAL RESERVOIR FORMATIONS."

[49] D. Whitfill, "Lost Circulation Material Selection, Particle Size Distribution and Fracture Modeling with Fracture Simulation Software," *Society of Petroleum Engineers - IADC/SPE Asia Pacific Drilling Technology Conference 2008 - "Drilling Technology to Access Future Energy Demand and Environmental Challenges,"* pp. 382–393, Aug. 2008, doi: 10.2118/115039-MS.

[50] K. Bybee, "Wellbore-Strengthening Technique for Drilling Operations," *Journal of Petroleum Technology*, vol. 60, no. 01, pp. 67–70, Jan. 2008, doi: 10.2118/0108-0067-JPT.

[51] F. E. Dupriest, "Fracture Closure Stress (FCS) and Lost Returns Practices," *All Days*, Feb. 2005, doi: 10.2118/92192-MS.

[52] A. K. Salih and H. A. Abdul Hussein, "Lost Circulation Prediction Using Decision Tree, Random Forest, and Extra Trees Algorithms for an Iraqi Oil Field," *Iraqi Geological Journal*, vol. 55, no. 2, pp. 111–127, Nov. 2022, doi: 10.46717/IGJ.55.2E.7MS-2022-11-21.

[53] S. Barrett, J. P. Cassanelli, G. Manescu, G. Vasquez, and F. Growcock, "Wellbore Strengthening – Where Field Application Meets Theory," *SPE Latin American and Caribbean Petroleum Engineering Conference Proceedings*, vol. 2, pp. 1082–1093, Dec. 2010, doi: 10.2118/139167-MS.

[54] M. G. Temraz and I. Hassanien, "Mineralogy and rheological properties of some Egyptian bentonite for drilling fluids," *J Nat Gas Sci Eng*, vol. 31, pp. 791–799, Apr. 2016, doi: 10.1016/J.JNGSE.2016.03.072.

[55] D. Skban Ibrahim, N. Amer Sami, and N. Balasubramanian, "Effect of barite and gas oil drilling fluid additives on the reservoir rock characteristics", doi: 10.1007/s13202-016-0258-2.

[56] "Experiments on the abrasion of casings by barite and iron ore powders | Request PDF." https://www.researchgate.net/publication/289588590_Experiments_on_the_abrasion_of_casings_by_barite_and_iron_ore_powders (accessed May 02, 2023).

[57] T. Kasikowski, R. Buczkowski, and M. Cichosz, "Utilisation of synthetic soda-ash industry by-products," *Int J Prod Econ*, vol. 112, no. 2, pp. 971–984, Apr. 2008, doi: 10.1016/J.IJPE.2007.08.003.

[58] V. C. Kelessidis, E. Poulakakis, and V. Chatzistamou, "Use of Carbopol 980 and carboxymethyl cellulose polymers as rheology modifiers of sodium-bentonite water dispersions," *Appl Clay Sci*, vol. 54, no. 1, pp. 63–69, Nov. 2011, doi: 10.1016/J.CLAY.2011.07.013.

[59] "POLYPAC R Polyanionic-Cellulose Filtration-Control Additive | SLB." https://www.slb.com/products-and-services/innovating-in-oil-and-gas/drilling/drilling-fluids-and-well-cementing/drilling-fluids/drilling-fluid-additives/filtration-reducers/polypac-r-filtration-control-additive (accessed Jun. 06, 2023).

[60] "GTL Solvents Product Stewardship Summary," 2022. [Online]. Available: http://www.reachcentrum.eu/en/consortiumslt/consortia-under-reach/hydrocarbon-solvents-

[61] Q. Wang *et al.*, "Lubricity and Rheological Properties of Highly Dispersed Graphite in Clay-Water-Based Drilling Fluids," *Materials 2022, Vol. 15, Page 1083*, vol. 15, no. 3, p. 1083, Jan. 2022, doi: 10.3390/MA15031083.

[62] "Petrochemicals | Viscosity Measurement of Drilling Fluids with RheolabQC :: Anton-Paar.com." https://www.anton-paar.com/corp-en/services-support/document-

finder/application-reports/petrochemicals-viscosity-measurement-of-drilling-fluids-with-rheolabqc/ (accessed Jun. 08, 2023).

[63] A. Torsvik and J. Frøyen, "An new method for determining the effect of gas influx on petroleum related fluids Conference Paper · April 2013 CITATIONS 0 READS 180," 20014. [Online]. Available: https://www.researchgate.net/publication/265389677

[64] M. Toroqi and S. Vahidreza, "Experimental Analysis and Mechanistic Modeling of Wellbore Strengthening," Oct. 2012, doi: 10.11575/PRISM/26049.

8 Appendix

Number of Peaks

1. Test 1 (quartz performance)

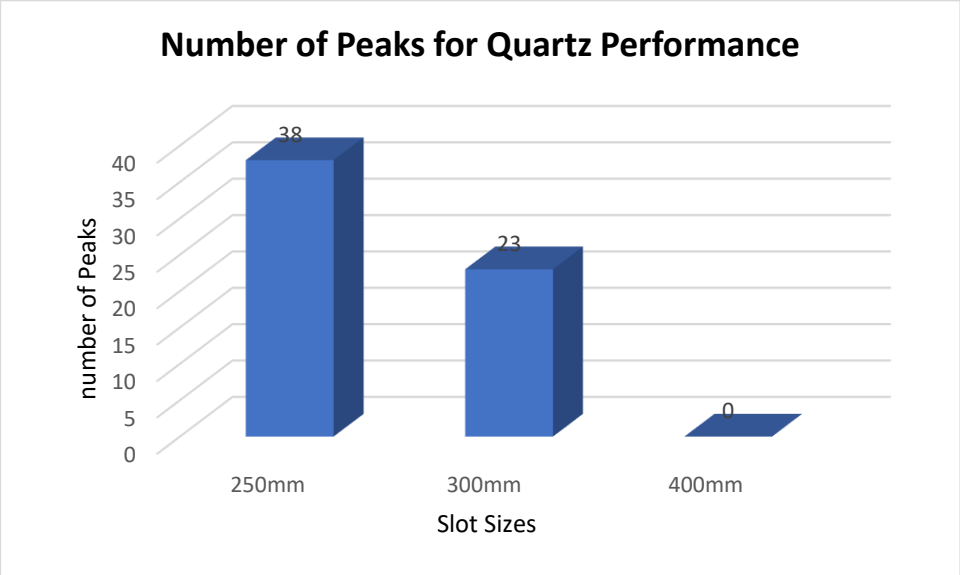

2. Test 2 (effect of Viscosity)

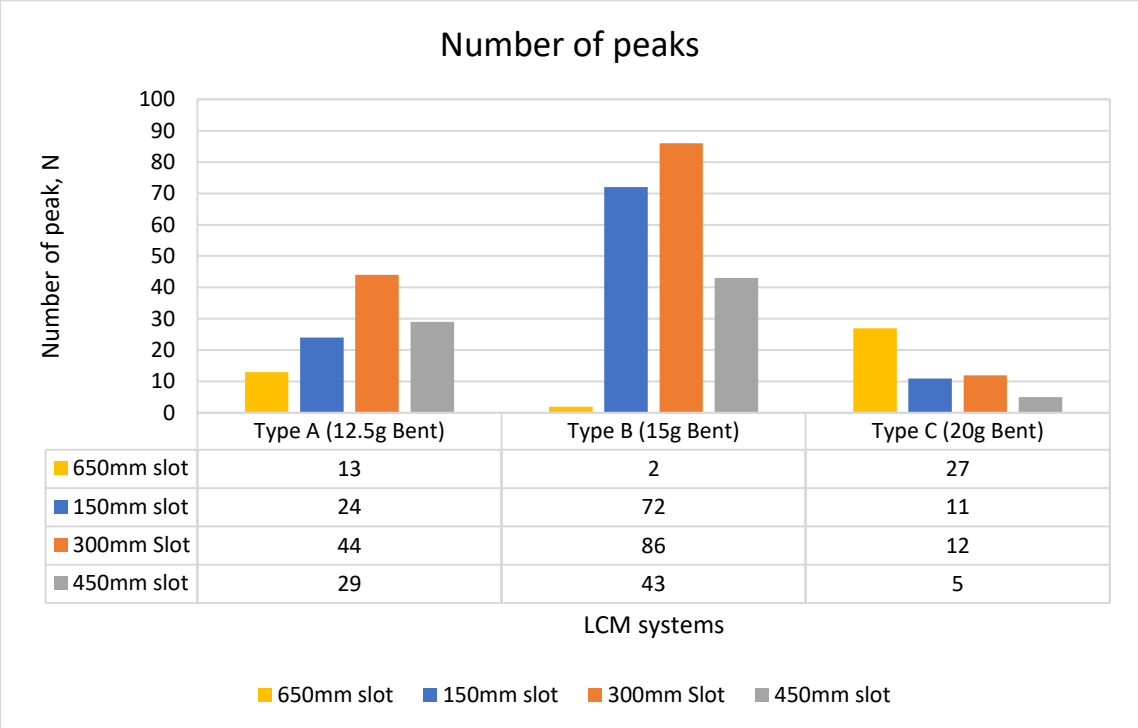

	Type A (12.5g Bent)	Type B (15g Bent)	Type C (20g Bent)
650mm slot	13	2	27
150mm slot	24	72	11
300mm Slot	44	86	12
450mm slot	29	43	5

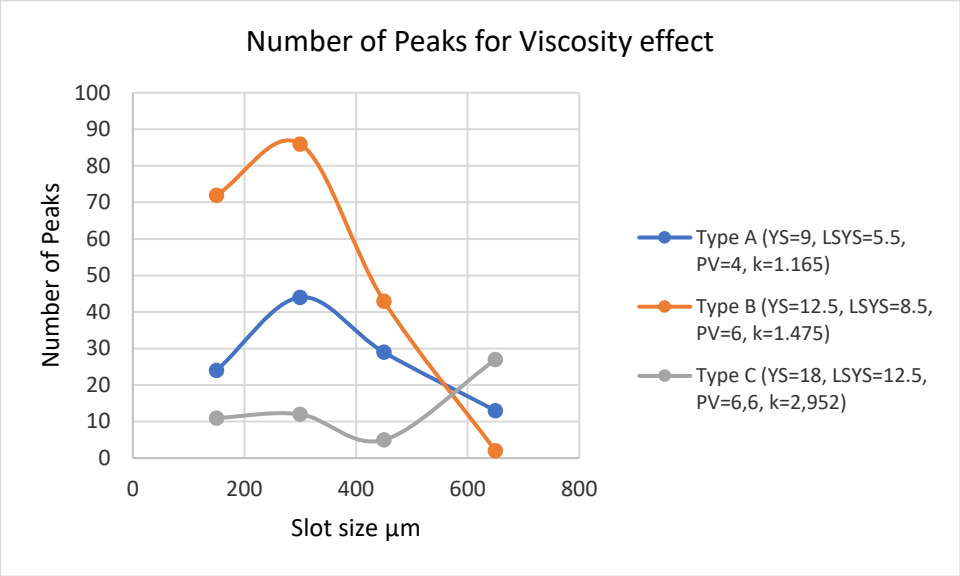

3. Test 3 (effect of Lubricity)

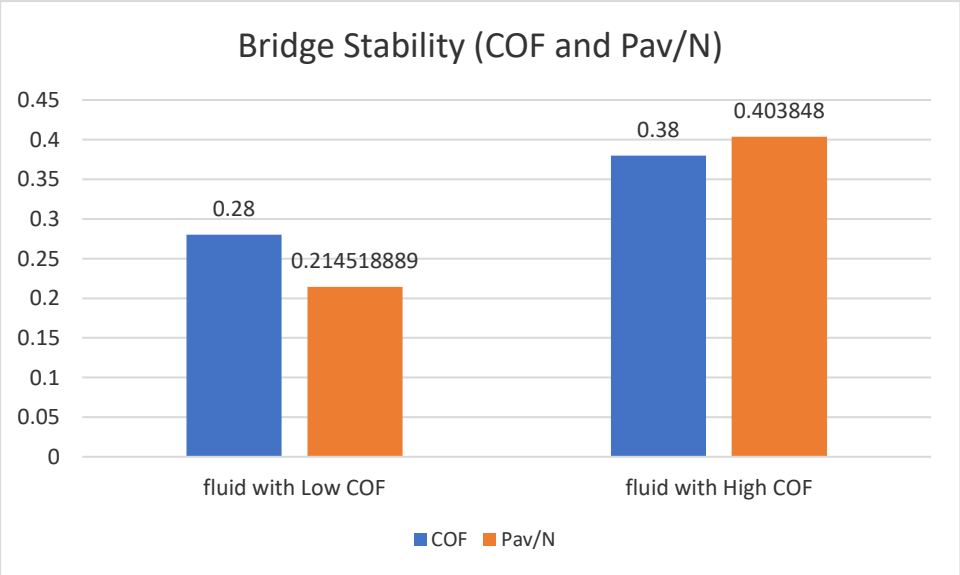

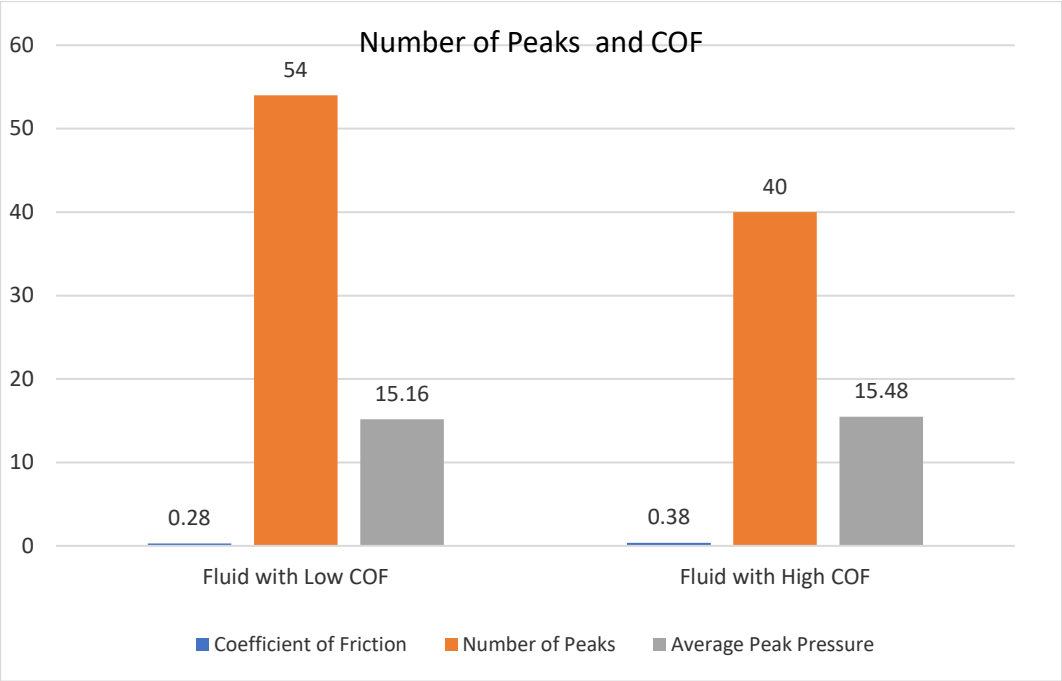

Stress Cage

In shales the bridge must be virtually impermeable to avoid fracture propagation:

Impermeable/no leak off

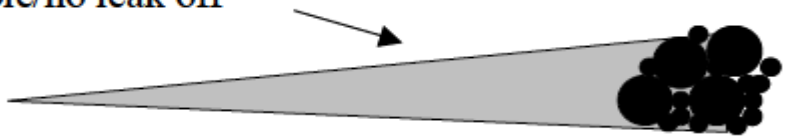

In permeable formations such as sands the bridge can be imperfect as pressure can leak away into the rock: